Fuel, Volume 388, May 2025, Article number 134469
DOI:10.1016/j.fuel.2025.134469

A Comparative Techno-Economic Feasibility of Hydrogen Production from Sugarcane Bagasse and Bread Waste

Rendra Hakim Hafyan[a], Jhuma Sadhukhan[b], Vinod Kumar[c], Sunil K. Maity[d] Siddharth Gadkari[a,*]

[a] *School of Chemistry and Chemical Engineering, University of Surrey, Guildford GU2 7XH, UK*

[b] *Centre for Environment & Sustainability (CES), School of Sustainability, Civil and Environmental Engineering, University of Surrey, Guildford GU2 7XH, UK*

[c] *Faculty of Engineering and Applied Sciences, Cranfield University, Cranfield MK43 0AL, UK*

[d] *Department of Chemical Engineering, Indian Institute of Technology Hyderabad, Kandi, Sangareddy 502284, Telangana, India*

Abstract

An increase in the emphasis on sustainable energy solutions underscores a vital need for hydrogen as a clean, decarbonizing, and efficient energy carrier. This necessity is driving extensive research into alternative feedstocks for hydrogen production. Promising resources like sugarcane bagasse and bread waste, valued for their abundance and high sugar content, can be a promising feedstock for hydrogen. Processes, such as steam reforming of ethanol and aqueous-phase reforming of xylitol, effectively utilize sugarcane bagasse and bread waste to produce hydrogen, supporting a circular bioeconomy and reducing dependence on fossil fuels. This study aims to investigate the process design and techno-economic feasibility of hydrogen production from sugarcane bagasse and bread waste. Results show that sugarcane bagasse-based feedstock requires higher capital investment and annual operational costs, at 68.3 M$ and 24.3 M$ per year compared to bread waste-based feedstock, which involves 49.8 M$ and 18.74 M$ per year, respectively. Profitability analysis indicated that bread waste-based hydrogen production was more economically viable, with a higher net present value of 36.45 M$ and a higher internal rate of return of 17%, along with a payback period of 11 years. A sensitivity analysis revealed that the selling price of hydrogen and fixed capital investment were the most

Published by Elsevier. This is the Author Accepted Manuscript issued with: Creative Commons Attribution License (CC:BY 4.0).
The final published version (version of record) is available online at DOI:10.1016/j.fuel.2025.134469. Please refer to any applicable publisher terms of use.

influential parameters affecting net present value. These findings highlight the economic advantages of utilizing bread waste over sugarcane bagasse, suggesting that bread waste is a more cost-effective and sustainable option for hydrogen production. By prioritizing bread waste as a feedstock, it is possible to achieve significant economic benefits, making it a strategic choice for future hydrogen production initiatives and advancing renewable energy technologies.

1. Introduction

Global energy consumption is anticipated to increase by nearly 50% by 2050, driven by robust economic growth and escalating demand, particularly from developing regions in Asia [1]. The industrial sector is projected to witness over 30% growth in energy use during this period [2]. Currently, fossil fuels supply about 80% of global energy demand, resulting in significant negative environmental impacts, notably through carbon dioxide emissions, a primary greenhouse gas (GHG) [3]. To combat these issues, a shift to lower-carbon energy sources with high energy density is strongly encouraged. This transition is not only expected to meet the increasing energy demand but also to drive technological advancements and mitigate the impacts of climate change. Therefore, decarbonizing the energy sector is vital for achieving sustainable economic growth and preserving environmental health. Hydrogen (H_2), stands out as a promising energy source, offering high energy density (120-142 MJ/kg) and producing zero emissions at the point of use [4]. As a versatile energy carrier, H_2 is instrumental in decarbonizing high-emission sectors, including chemical production (especially methanol and ammonia/urea), oil refining, electronics, oil and fat hydrogenation, and metal and glass manufacturing [5]. Moreover, H_2 is a clean fuel for combustion processes, generating only water vapor [6]. Given its potential, the H_2 market is expected to expand significantly, with annual growth rates of 5-10%, reaching 100 million tons by 2024 [6, 7].

Currently, 96% of H_2 production is derived from fossil fuels, with 48% via steam methane reforming (SMR), 18% through coal gasification, and 30% by partial oxidation of oil [4, 8]. China dominates global H_2 production at 34%, followed by Middle East at 15%, North America at 10%, India at 9%, and Europe at 6% [7]. The SMR is still preferable due to reduced process complexity with a low production cost

(0.75 $/kg) even though it releases a high amount of CO_2, around 10-12 kg CO_2/kg H_2 produced [3, 6, 9]. However, the cost of H_2 production is expected to decline significantly in the future, driven by technological advancements and increased deployment. In the IEA's Net Zero Emissions by 2050 Scenario (NZE Scenario), the cost of low-emission H_2 from renewable electricity is projected to fall to 2-9 USD/kg H_2 by 2030—half of today's value—narrowing the cost gap with unabated fossil-based production from 1.5-8 USD/kg H_2 today to 1-3 USD/kg H_2 by 2030 [7]. H_2 produced by conventional processes is referred to as "grey H_2," which uses fossil resources without carbon mitigation. In contrast, "blue H_2" is produced using the same methods but incorporates carbon capture and storage (CCS), while "green H_2" is produced via water electrolysis powered by renewable energy sources, such as solar PV or wind power[10]. The trend of reducing technology costs and improving efficiency is making green H_2 from water electrolysis increasingly competitive with fossil fuel-based methods. María Villarreal Vives, et al. [11] demonstrated that integrating a 10 MW proton exchange membrane electrolyser with heat recovery and an organic Rankine cycle (ORC) improved efficiency from 71.4% to 98%, though it remains economically unviable at low electricity prices due to additional costs. Shaner, et al. [12] found that photoelectrochemical (PEC) systems for solar H_2 production had lower transport costs and were more economically favourable than photovoltaic-electrolytic (PV-E) systems, with the levelized cost of H_2 (LCOH) for PEC systems estimated at 11.4 $/kg and 9.2 $/kg for non-concentrating and concentrating systems, respectively. Henry, et al. [13] showed that H_2 production from wind using commercially available desalination and electrolysis units was economically competitive with natural gas-derived H_2 at larger scales, with a minimum selling price of 6.40 $/kg. Alkaline electrolysers were found to produce cheaper H_2 than proton exchange membrane electrolysers. Liponi, et al. [14] revealed that an alkaline electrolyser powered by a 1 MW photovoltaic plant achieves the lowest LCOH with an intermediate nominal power of 0.2 MW, given an electricity price of 106.27 $/MWh. However, larger electrolyser sizes led to higher capital costs that were not offset by increased H_2 production. These studies offer valuable insights and significant improvements, providing optimism for replacing SMR in the future. Nonetheless, the sustainability of green H_2 is

closely tied to the electricity source used for its production. Additionally, the dominant reliance on fossil fuel-based feedstocks for H_2 production raises environmental concerns, including the depletion of fossil fuels [15]. Recent research emphasizes the need for alternative feedstocks, such as waste biomass—including food waste and lignocellulosic biomass—which are often underutilized or mismanaged [16].

Biomass is abundant, low-cost, and carbon-neutral, making it a sustainable resource for replacing fossil fuels [3, 17]. It can be used as a feedstock for H_2 production and has been extensively studied for technological development. Promising biomass utilization technologies for H_2 production include gasification [18], pyrolysis [19], and emerging technologies, such as photocatalytic processes [20], biological water-gas shift reaction [21], and dark fermentation [22]. Among the various feedstocks, sugarcane bagasse (SCB) and bread waste (BW) are particularly promising due to their abundance and high sugar content. SCB, a byproduct of sugarcane juice extraction, constitutes 25-30% of sugarcane on a wet basis [23]. It is composed of 40-42% cellulose, 28-30% hemicellulose, and 18-20% lignin [24]. Major sugarcane producers, such as India and Brazil, generate substantial quantities of SCB, with India alone producing about 100 million tons annually [25]. Currently, SCB is primarily used for cogeneration in heat and power production, contributing to the sugar industry's energy self-sufficiency and generating revenue from excess sales [26]. Similarly, BW is a significant waste product in Europe, with large quantities discarded each year. Countries like Sweden (80,410 tons), Denmark (30,000 tons), France (640,000 tons), Germany (1,700,000 tons), the Netherlands (120,000 tons), Spain (60,000 tons), and Turkey (680,000 tons) produce substantial amounts of BW annually [27, 28]. In the UK alone, approximately 20 million slices of bread are wasted daily, contributing to 292,000 tons of annual waste and 584,000 tons of CO_2-equivalent emissions [29]. BW is composed of 50-70% starch, 8-10% protein, and 1-5% fat [30]. Due to its high glucose content, BW has been widely studied for converting into value-added products such as bioethanol [31], succinic acid [32], lactic acid [33], and 2,3-butanediol [34]. Utilizing these feedstocks for bioenergy production supports a circular bioeconomy by effectively managing waste and reducing reliance on fossil fuels.

H_2 production from biomass using steam reforming of ethanol (SRE) and aqueous-phase reforming (APR) is gaining significant attention as a sustainable and renewable energy solution. SRE involves the conversion of bioethanol, derived from biomass, into H_2. Ethanol-based feedstocks are advantageous because it is less hazardous than methanol and can be produced from diverse biomass sources [35]. This versatility has made ethanol an attractive option for many researchers performing catalyst development, with experimental studies in SRE exploring various catalysts such as Rh/Co Ferencz, et al. [36], Ni/Al_2O_3 [37], Ni/CeO2-ZrO2 [38], Rh/CeO2/γ-Al2O3 [39]. In addition, some studies have performed the economic evaluation of SRE. Compagnoni, et al. [40] evaluated a large-scale SRE plant and their analysis showed a net present value (NPV) of 50.8 M$ over 30 years, with internal rate return (IRR) of 24.9% and a payback period (PBP) of 7.3 years. They emphasized the process's sensitivity to ethanol feedstock costs and H_2 selling prices. Moraes, et al. [41] found that producing H_2 at 8.87 $/kg using Brazilian ethanol priced at 0.81 $/L was competitive with California market prices of 13.44 $/kg. Khamhaeng, et al. [42] compared steam reforming and dehydrogenation of ethanol for H_2 production, finding steam reforming the most cost-effective at $1.58/kg H_2. They noted that dehydrogenation produced byproducts like ethyl acetate and acetaldehyde, negatively affecting CO_2 emissions per ton of methanol converted. While the above studies demonstrate the economic potential of SRE for H_2 production, they also highlight the significant impact of bioethanol feedstock costs on the overall economic feasibility. In addition to SRE, APR is another process for producing H_2, particularly from polyols like xylitol derived from lignocellulosic biomass, which serve as key feedstocks for the process. The APR process operates under mild conditions and moderate pressures [43]. Other advantages include the use of water as a green solvent and the elimination of feedstock vaporization [44]. Similar to SRE, many studies have focused on catalyst development for the APR process, exploring catalysts such asPt/HZSM-5 and Ni/HZSM-5 catalysts [45], Pt/C and Pt/TiC-CDC [46], Pt/Al_2O_3 catalysts [47], Pt/C [48], and Pt-Re[49]. Additionally, a few studies have conducted economic assessments of APR. For example, Khodabandehloo, et al. [50] performed a techno-economic evaluation of hydrogen production through glycerol reforming in aqueous phase, estimating the total cost of H_2 production at

7.45 $/kg. Similarly, Sladkovskiy, et al. [51] reported that the cost of producing H_2 from sorbitol ranged from 12.94 to 13.58 $/kg.

SCB stands out as a highly versatile feedstock due to its composition, which includes high cellulose content that can be converted into glucose (a precursor for ethanol) and xylose (a precursor for xylitol). This dual capability makes SCB suitable for both SRE and APR processes. In SRE, ethanol derived from glucose undergoes reforming to produce H_2, while in APR, xylitol from xylose serves as an efficient precursor for H_2 production On the other hand, BW, while an excellent source of carbohydrates, is more limited in its application. Its carbohydrate content primarily yields glucose, which can be converted into ethanol for use in SRE to produce H_2. Despite the promising potential of renewable biomass feedstocks like SCB and BW, a critical gap remains in the literature regarding comprehensive economic assessments of H_2 production using SRE or APR from biomass. Understanding their economic potential is crucial as these technologies remain in early-stage, small-scale development, presenting a novel area for future research and development.

The main objective of this study is to investigate the technical and techno-economic performance of H_2 production from SCB and BW. Our study aims to fill the existing gap by evaluating the economics of H_2 production from these feedstocks. Specifically, this research addresses the questions: How does the process performance of H_2 production from SCB compare to that from BW?; What is the economic potential of using SCB and BW for H_2 production? We conducted comprehensive techno-economic analyses focusing on H_2 productivity, capital investments, operating costs, and H_2 profitability. Key economic metrics, such as NPV, IRR, and PBP, are estimated to determine overall profitability. Additionally, the study considers the secondary benefits of using biomass for H_2 production, as other components, such as lignin in SCB and proteins and lipids in BW, can be utilized for energy generation (electricity and heat). Furthermore, our study integrates co-generation for energy generation and a carbon capture unit (CCU) into the H_2 production processes. This holistic approach not only aims to enhance the economic viability of H_2 production from SCB and BW but also seeks to maximize the utilization of all biomass components, contributing to a more sustainable and efficient energy system.

Nomenclature

Abbreviations

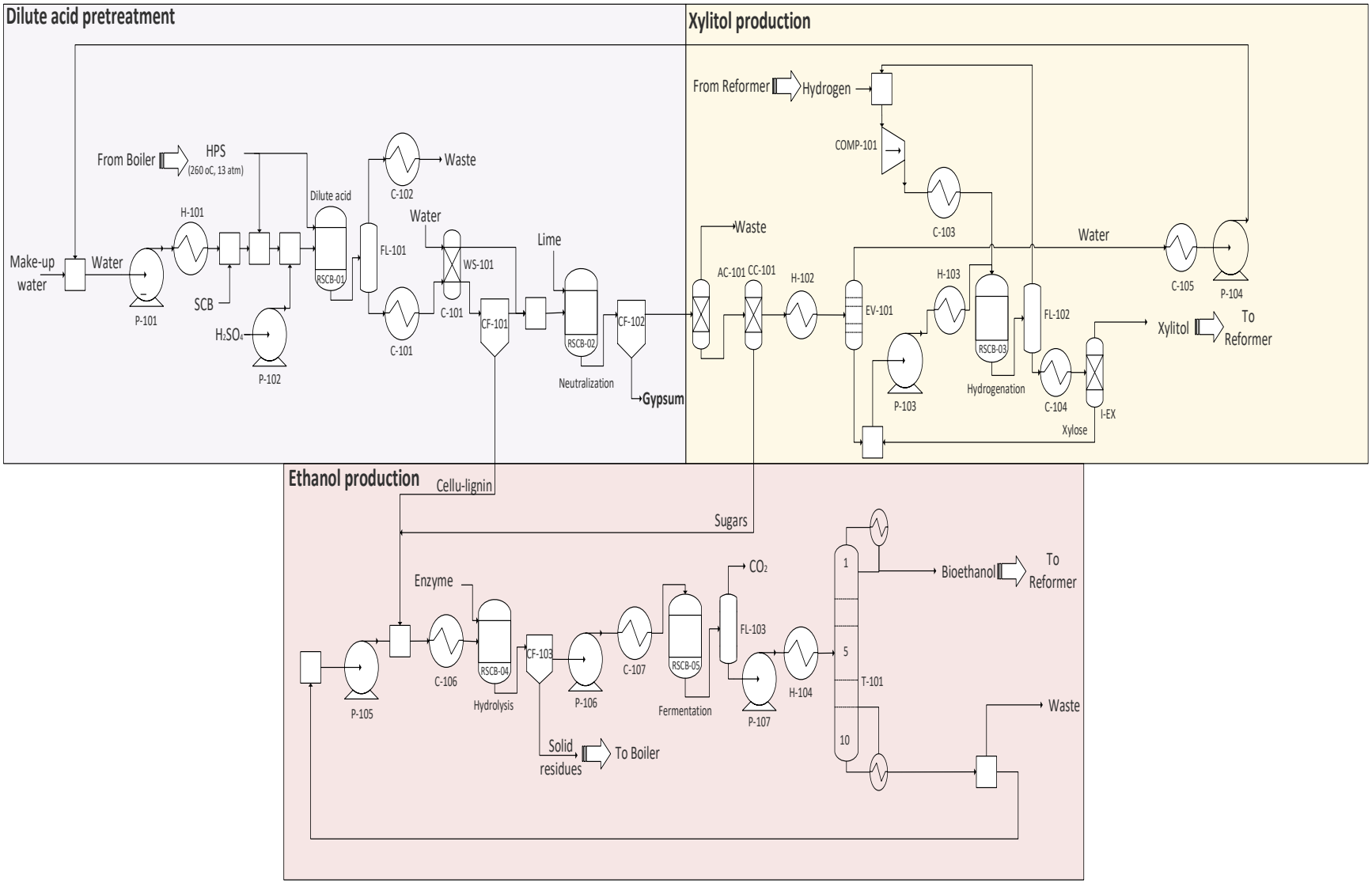
GHG	greenhouse gas
SMR	steam methane reforming
CCS	carbon capture storage
ORC	organic rankine cycle
PEC	photoelectrochemical
LCOH	levelized cost of H_2
SCB	sugarcane bagasse
BW	bread waste
SRE	steam reforming of ethanol
APR	aqueous-phase reforming
NPV	net present value
IRR	internal rate return
PBP	payback period
WGS	water-gas shift
NRTL	non-random two liquid
NREL	national renewable energy laboratory
AD	anaerobic digestion
HPS	high pressure steam
LPS	low pressure steam
GAC	granular activated carbon
HT-WGS	high temperature water gas shift

LT-WGS	low temperature water gas shift
HEN	heat exchanger network
CAPEX	capital expenditure
OPEX	operational expenditure

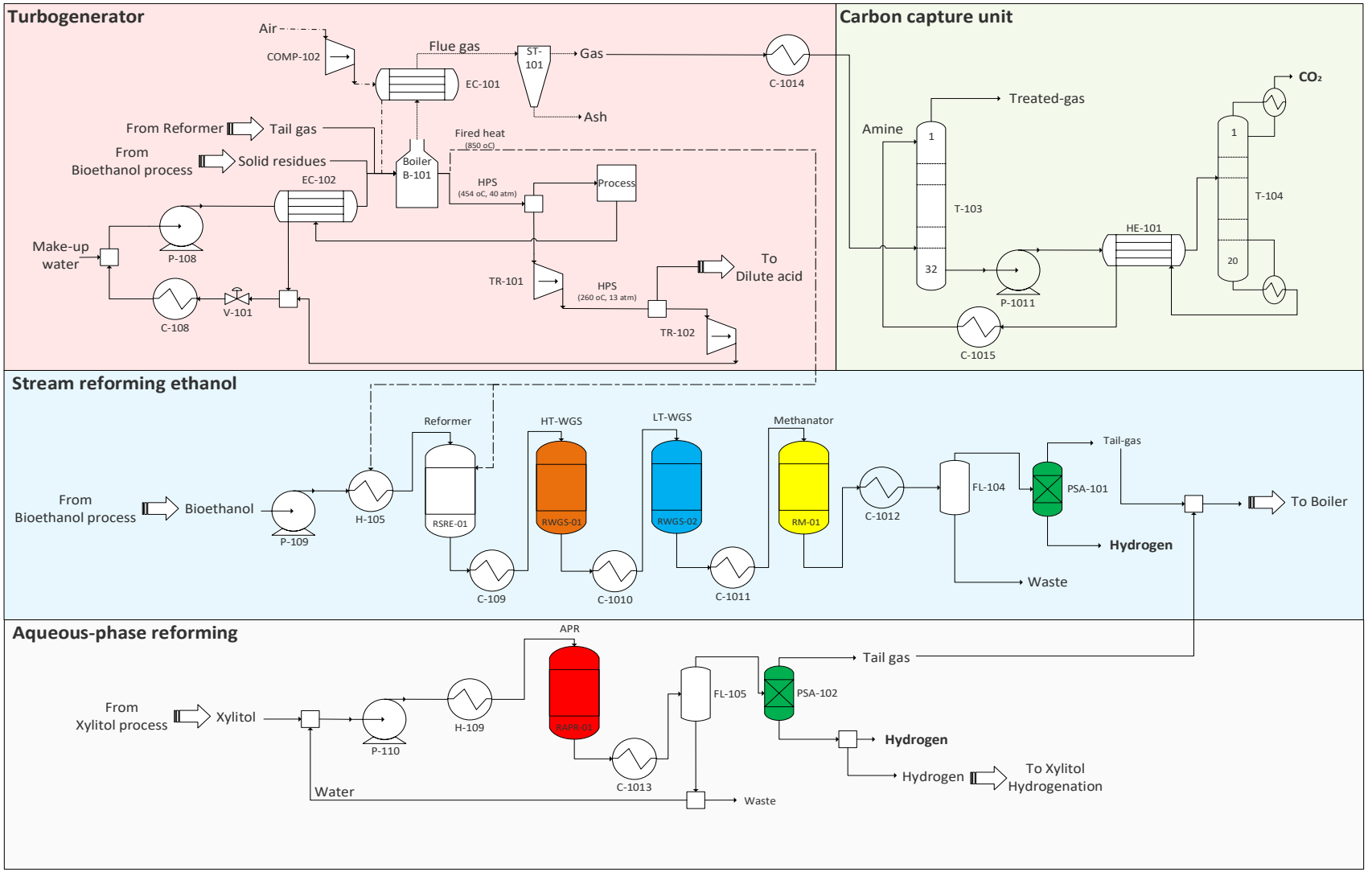
2. Material and method

This study investigates the potential of H_2 production from biomass by focusing on the feedstocks SCB and BW. SCB contains 35% moisture content, with its dry chemical composition comprising 48.5% cellulose, 21% hemicellulose, 18% lignin, 3.4% ash, and 9.1% other solids [23]. In contrast, BW consists of 46 wt% starch, 7.9 wt% protein, 2 wt% fat, 2.5 wt% fiber, 1 wt% salt, and 40.6 wt% water [31]. A capacity of 100 MT/day for both feedstocks is modeled using Aspen Plus V.11 to assess the techno-economic performance of H_2 production. The simulation employs the Non-Random Two-Liquid (NRTL) thermodynamic model, which is specifically suited for non-ideal biomass systems [52]. This model is widely recognized for its accuracy in predicting phase behavior, such as liquid-liquid and liquid-vapor equilibria, as well as key transport properties, including mole fractions and activity coefficients [53]. For the reforming processes, including SRE and APR, the Soave-Redlich-Kwong (SRK) property package is utilized, given its proven reliability in hydrocarbon processing simulations [37, 54]. Additionally, the acid gas-chemical solvents package is employed for modelling the carbon capture process [27]. The stream class in the simulation is designated as MIXCISLD, enabling component specifications as either conventional substances or solids without requiring particle size distribution. Component and thermophysical properties for lignocellulosic materials are sourced from the Aspen Plus database and the National Renewable Energy Laboratory (NREL) database [55]. Mass and energy balances derived from the simulation inform equipment sizing, cost estimation, and overall economic assessments. This study evaluates two distinct process scenarios for H_2 production from SCB and BW, with each scenario modeled as a standalone facility to enable comparative analysis.

- Scenario 1 (SC-1): This scenario outlines a self-contained facility dedicated to H_2 production using SCB. The detailed process flow diagram is illustrated in Fig. 1. At the beginning, SCB involves a series of preprocesses aimed at extracting hemicellulose and cellulose. The xylose rich hemicellulosic fraction is utilized in the production of xylitol from xylose via a chemical hydrogenation process while the cellulosic fraction is employed for the synthesis of bioethanol through enzymatic hydrolysis to glucose and subsequent fermentation. Subsequently, H_2 is derived from xylitol using APR, while ethanol is converted through the SRE process. The solid residues, primarily composed of lignin, separated during bioethanol production, are combusted in a boiler alongside tail gas resulting from the steam reforming process to generate energy in the form of heat and electricity. The generated energy is employed to fulfil the energy demands within the plant. The flue gas emitted during the combustion process is subjected to CCU to cut down carbon emissions. Additionally, pinch technology is employed to systematically enhance energy efficiency and reduce operating costs.
- Scenario 2 (SC-2): In this scenario, BW serves as the primary feedstock for H_2 production, as the process can be seen in Fig. 2. The process commences with BW undergoing sequential hydrolysis of starch to glucose and fermentation. The fermentable sugars obtained from hydrolysis are metabolized by *S. cerevisiae KL17* microorganisms to yield bioethanol. The resulting bioethanol is then separated from the fermentation mixture downstream. This bioethanol is subsequently fed into the SRE process, yielding H_2 as the primary product along with tail gas. The residual waste fraction from bioethanol production, primarily consisting of protein and fat, undergoes anaerobic digestion (AD), leading to the production of biogas. The biogas, along with the tail gas, serves as an energy source for the boiler unit, effectively meeting the energy requirements of the entire process, including both heat and electricity demands. Furthermore, this scenario incorporates the utilization of the CCU and pinch technology to cut down CO_2 emissions and energy demands, respectively.


Dilute acid pretreatment
Xylitol production
Ethanol production
From Boiler
HPS
(260 oC, 13 atm)
Waste
C-102
Dilute acid
H-101
Water
Lime
Make-up water
Water
FL-101
WS-101
RSCB-01
SCB
P-101
H_2SO_4
P-102
C-101
C-101
CF-101
RSCB-02
CF-102
Neutralization
Gypsum
From Reformer
Hydrogen
COMP-101
C-103
Waste
Water
AC-101
CC-101
H-102
H-103
C-105
P-104
EV-101
RSCB-03
FL-102
Xylitol
To Reformer
P-103
Hydrogenation
C-104
I-EX
Xylose
Cellu-lignin
Sugars
Enzyme
CO_2
Bioethanol
To Reformer
C-106
RSCB-04
Hydrolysis
CF-103
P-106
C-107
RSCB-05
Fermentation
FL-103
P-107
H-104
T-101
1
5
10
P-105
Solid residues
To Boiler
Waste

(a)


Turbogenerator
Air
COMP-102
Flue gas
EC-101
ST-101
Gas
Ash
C-1014
From Reformer
Tail gas
From Bioethanol process
Solid residues
Fired heat (850 oC)
Boiler B-101
HPS (454 oC, 40 atm)
Process
EC-102
Make-up water
P-108
C-108
V-101
TR-101
HPS (260 oC, 13 atm)
To Dilute acid
TR-102
Carbon capture unit
Amine
Treated-gas
T-103
1
32
P-1011
C-1015
HE-101
T-104
CO2
Stream reforming ethanol
From Bioethanol process
Bioethanol
P-109
H-105
Reformer
RSRE-01
HT-WGS
RWGS-01
LT-WGS
RWGS-02
Methanator
RM-01
C-1012
FL-104
PSA-101
Tail-gas
To Boiler
Hydrogen
Waste
C-109
C-1010
C-1011
Aqueous-phase reforming
From Xylitol process
Xylitol
P-110
H-109
APR
RAPR-01
C-1013
FL-105
PSA-102
Tail gas
Hydrogen
Hydrogen
To Xylitol Hydrogenation
Water
Waste

(b)

Fig. 1. Process flow diagram of H_2 production from SCB. (a) dilute acid pretreatment with xylitol and ethanol production; (b) APR, SRE, turbogenerator, and CC unit.

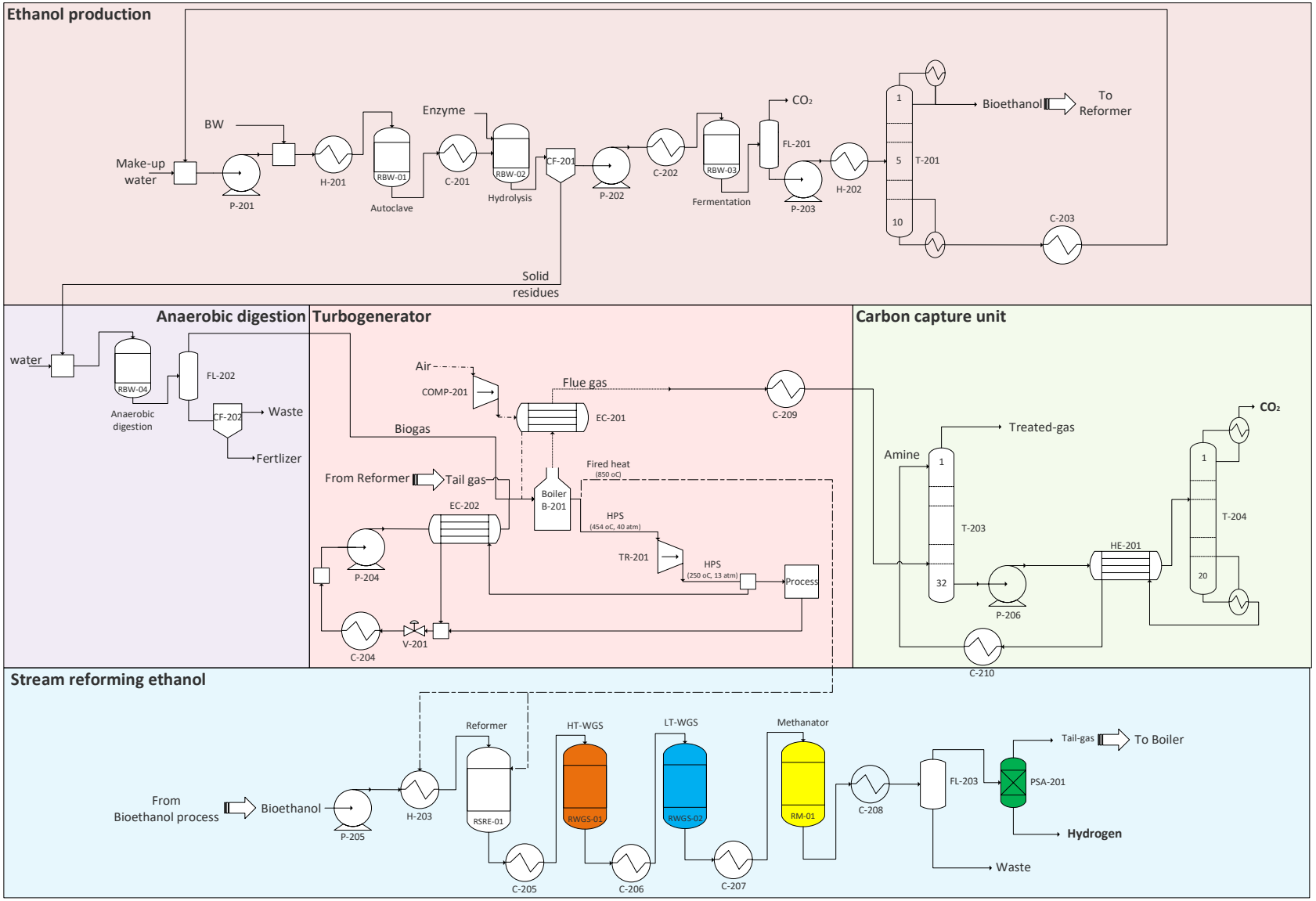

Ethanol production
BW
Make-up water
P-201
H-201
RBW-01
Autoclave
C-201
Enzyme
RBW-02
Hydrolysis
CF-201
P-202
C-202
RBW-03
Fermentation
CO₂
FL-201
P-203
H-202
1
5
10
T-201
Bioethanol
To Reformer
C-203
Solid residues
Anaerobic digestion
water
RBW-04
Anaerobic digestion
FL-202
CF-202
Waste
Fertlizer
Turbogenerator
Air
COMP-201
Flue gas
EC-201
C-209
Biogas
From Reformer
Tail gas
Fired heat
(850 oC)
Boiler B-201
EC-202
HPS
(454 oC, 40 atm)
TR-201
HPS
(250 oC, 13 atm)
Process
P-204
C-204
V-201
Carbon capture unit
Amine
Treated-gas
1
32
T-203
P-206
HE-201
1
20
T-204
CO₂
C-210
Stream reforming ethanol
From Bioethanol process
Bioethanol
P-205
H-203
Reformer
RSRE-01
C-205
HT-WGS
RWGS-01
C-206
LT-WGS
RWGS-02
C-207
Methanator
RM-01
C-208
FL-203
PSA-201
Tail-gas
To Boiler
Hydrogen
Waste

Fig. 2. The process flow diagram of H_2 production from BW.

2.1. Process design

2.1.1. SCB valorisation process to xylitol and ethanol

The process begins with the pretreatment with dilute acid (DA), where SCB is mixed with hot water to form a slurry with solids loading aimed at controlling the pretreatment effluent at levels of 30 wt% total solids [55]. Following this, the mixture is preheated to 135°C using high-pressure steam (HPS) and then fed into the reactor (RSCB-01) along with dilute H_2SO_4 at a ratio of 18 mg/g of dry SCB. The reactor is maintained at 156 °C and 5 bar by injecting HPS directly into it, allowing pressurized steam to flow through solids and generate two intermediate streams: the liquid fraction, known as hydrolysate, primarily containing xylose rich solubilized and hydrolysed solids, mostly hemicellulose, while the solid fraction left in the reactor after pretreatment, referred to as residue, mainly consists of cellulose and insoluble lignin [56]. After 5 minutes, the reactor contents undergo rapid cooling to atmospheric conditions to facilitate excess water removal. Subsequently, the generated vapor is used to preheat incoming water, optimizing energy utilization within the process [57, 58]. Next, the hydrolysate stream is cooled to 50°C and filtered using a filter press to separate the liquid hydrolysate from the cellu-lignin residual material. Any remaining acid and hydrolysate in the solid stream are washed before enzymatic hydrolysis [23]. The moisture in the filtered solids is washed with water fed at a rate of 1 g water per 1 g dry matter [58]. The soluble hemicellulose hydrolysate fraction is then treated with lime to neutralize (RSCB-02) the sulfuric acid used during DA treatment and prevent possible downstream catalyst deactivation. The resulting calcium sulphate (gypsum) precipitate is recovered using filtration, and the xylose rich free from H_2SO_4 stream is directed to xylitol production.

Xylitol production involves the conversion of hydrolysed hemicellulose (xylose) from the pretreatment into xylitol through chemical hydrogenation. After the pretreatment stage, the chemical route for xylitol production comprises three stages: xylose purification, catalytic hydrogenation, and xylitol purification. To utilize xylose further, the neutralized hydrolysed material containing inhibitors is directed to a granular activated carbon (GAC) column to eliminate furfural completely with minimal sugar loss [58]. The liquid hydrolysate stream, containing pentose and hexose sugars from dilute acid

hydrolysis and GAC detoxification, undergoes ion-exchange chromatography to separate pentose sugar from hexose sugars. It is assumed that glucose and arabinose are completely removed in this process [58]. The resulting xylose stream is concentrated using an evaporator to achieve a 20% concentration. The hydrogenation of xylose takes place in the presence of Raney nickel catalyst at hydrogenation reactor (RSCB-03) with a loading of 5% (w/w) of xylose, known for its cost-effectiveness and high conversions with selectivity [59]. Maintaining a reaction slurry free of hexose sugar is crucial to avoid complicating downstream processes. H_2 gas pressurizes the reactor, maintained at 135°C and 40 atm for 2.5 hours. The unreacted H_2 is recycled to maintain a hydrogen-to-xylose ratio four times the stoichiometric requirement [60]. After 2.5 hours, 97% of xylose is converted to xylitol, with only 0.1% being converted to the by-product arabitol [58, 61, 62]. The xylose undergoes catalytic hydrogenation conversion into xylitol through the following reaction:

$$C_5H_{10}O_5 + H_2 \rightarrow C_5H_{12}O_5 \quad (1)$$

Upon exiting the reactor, the solution passes through a filter to recover the catalyst for recycling [63]. The effluent stream is then cooled to 65°C and purified using ion exchange membranes to remove all by-products. Unreacted xylose and by-products from the reaction process are recycled back into the reactor to enhance the overall yield of xylitol. During this process, a xylitol concentration of 20% by weight is achieved. This concentrated xylitol solution is then prepared to serve as feedstock for the APR stage. Meanwhile, the washed solids resulting from DA pretreatment are combined with water to form a slurry containing 20% solids before enzymatic hydrolysis. Cellulose hydrolysis is conducted at 50°C in enzymatic hydrolysis reactor (RSCB-04) for three days with an enzyme dosage of 20 g protein/kg dry mass, resulting in a 90% yield of glucose [58]. The slurry rich in glucose is then filtered to separate solid residues, which are directed to the boiler for energy generation. The liquid hydrolysate, abundant in glucose, undergoes processing for bioethanol production. The streams containing reducing sugars from previous stages are transformed into ethanol by a recombinant

bacterium, *Zymomonas mobilis*, at 33°C for 30 hours in fermenter (RSCB-05). The bioethanol fermentation is carried out according to the following reaction:

$$C_6H_{12}O_6 \xrightarrow{yeast} 2C_2H_5OH + 2CO_2 \quad (2)$$

This genetically engineered bacterium has the capability to utilize hexose as a carbon source, either solely or in combination with pentose. Following fermentation, the culture broth containing approximately 7-10% (w/w) ethanol [64] is directed to the separation zone. After fermentation, the broth containing approximately 7.5% ethanol by weight must be concentrated to prepare for the SRE process. The concentration process aims to achieve a water-to-ethanol (W/E) mole ratio of 5, which corresponds to an ethanol concentration of 33.86% by weight. Once this concentration is reached, the ethanol solution is pumped into the SRE system for further processing.

2.1.2. BW valorisation to ethanol and biogas production

This BW valorisation process is adapted from our previous work [27]. To prepare the BW for further processing, autoclaving is employed, eliminating the need for gelatinization and liquefaction steps. This process involves loading the BW into the autoclave (RBW-01) with an appropriate amount of water to form a slurry, which is then sealed and heated to a high temperature, typically between 121°C and 150°C, at a pressure of 1-3 bar. Under these elevated temperature and pressure conditions, complex carbohydrates and other organic compounds in the BW break down into simpler molecules, facilitating subsequent enzymatic hydrolysis. Additionally, autoclaving sterilizes the waste material, eliminating any potential harmful microorganisms. The resulting supernatant is cooled to 60°C and subjected to enzymatic hydrolysis (RBW-02) with the addition of *Dextrozyme Peak enzyme* for 48 hours, during which carbohydrates are converted into individual glucose molecules by the combined action of *amylase* and *amyloglucosidase enzymes*. Following enzymatic hydrolysis, the saccharified liquid, rich in sugars, is separated from other solid components and cooled to 32°C before fermentation (RBW-03) with Saccharomyces cerevisiae yeast, based on conditions derived from Narisetty, et al. [31]. After fermentation, the culture broth, which contains approximately 9% ethanol

by weight, is concentrated in a distillation column to 33.86% ethanol by weight. The concentrated ethanol solution is then pumped into the SRE process for further processing. Meanwhile, water-soluble organic streams from fermentation are sent to AD (RBW-04) for biogas production. The wastes are digested at 35°C for 10 days, with the generated biogas directed to the boiler unit for heat and electricity production. The remaining output generated in AD is then transferred to the dewatering to obtain solid and liquid digestate. The solid digestate substance containing around 25% dry solids (DS) [65]. The resulting digestate from AD serves as a valuable by-product, suitable for use as a fertilizer substitute [66].

2.1.3. H_2 production

2.1.3.1. APR

The simulation of the APR process is based on the experimental study conducted by Murzin, et al. [48], which provides data on conversion and selectivity for all reactions. In the simulation, the conversion reactor (RSTOIC) is modelled to represent the APR reactor (RAPR-01). The xylitol solution is pressurized to 22 bar and mixed with recycled water. This mixture is preheated to 225°C by a heater before entering the APR reactor. The APR of xylitol is carried out using a Pt/C catalyst, with the main products being H_2, CO_2, and a mixture of alkanes (primarily C1-C5) in the gas phase, along with oxygenated products in the liquid phase. The study focuses on gas phase products due to a lack of experimental data on liquid phase formation. Therefore, the formation products of APR primarily include H_2, CO_2, and alkanes, with propane being the dominant alkane. The formation of alkanes involves hydrodeoxygenation reactions with H_2 participation. The reactor is supplied with HPS to maintain isothermal conditions. After the reaction, the product stream from the reactor is cooled to 30°C to separate the gaseous products and water in the flash drum. Then, the gaseous stream is then directed to the pressure swing adsorption unit (PSA) for H_2 separation with a recovery rate of 85% [48].

2.1.3.2. SRE

The process for H_2 production through steam reforming of ethanol comprises a steam reformer, a high-temperature water gas shift (HT-WGS), a low-temperature water gas shift (LT-WGS), and methanation process. The kinetic model and reactions involved are sourced from various works listed in Table 1. The ethanol is pressurized to 20 bar and mixed with steam at a steam-to-ethanol molar ratio of 5. The mixture is heated to 650°C before entering the reactor (RSRE-01). The feed gas is introduced into the isothermal fixed-bed reactor on Ni/Al_2O_3 catalyst operating at 650°C and 20 bar [37]. The effluent gas is directed to WGS reactors in series to reduce CO content and increase H_2 production. The first reactor (RWGS-01) operates at 450°C, employing a power-law reaction rate expression for a commercial $Fe_2O_3/Cr_2O_3/CuO$ catalyst [67]. Meanwhile, the second reactor (RWGS-02) operates at 280°C employing a commercial $Cu/ZnO/Al_2O_3$ catalyst [68]. The outlet is further cooled to 210 °C before entering the methanation process (RM-01), where any remaining CO is converted into methane. Before entering the PSA, the stream is cooled to 35°C to condense most of the water present in the gas, with the condensate water removed in the flash drum. The PSA unit is employed to obtain pure H_2 and remove impurities, operating at 20 bar and 35°C, achieving H_2 purity of 99% [5].

Table 1. Major description of sub-processes in H_2 production processes.

Process	Description	Ref
APR of xylitol	Operating conditions: 225 °C and 22 bar Catalyst: Pt/C Conversion rate of xylitol to H_2: 80% Reaction mechanism: $C_5H_{12}O_5 \rightarrow 6H_2 + 5CO$ $CO + H_2O \rightarrow 5H_2 + 5CO_2$	Murzin, et al. [48]
SRE	Operating conditions: 650 °C and 20 bar Kinetic model: LHHW Catalyst: Ni/Al_2O_3	Rossetti, et al. [37]

	Reaction mechanisms: $CH_3CH_2OH \rightarrow CH_4 + CO + H_2$ (r_1) $CH_3CH_2OH + H_2O \rightarrow CO_2 + CH_4 + 2H_2$ (r_2) $CH_4 + H_2O \leftrightarrow CO + 3H_2$ (r_3) $CH_4 + 2H_2O \leftrightarrow CO_2 + 4H_2$ (r_4)	
HT-WGS	Operating conditions: 450 °C and 20 bar Kinetic model: Power Law Catalyst: $Fe_2O_3/Cr_2O_3/CuO$ Reaction mechanism: $CO + H_2O \leftrightarrow CO_2 + H_2$	Hla, et al. [67]
LT-WGS	Operating conditions: 280 °C and 20 bar Kinetic model: Power Law Catalyst: $Cu/ZnO/Al_2O_3$ Reaction mechanism: $CO + H_2O \leftrightarrow CO_2 + H_2$	Choi and Stenger [68]
Methanation	Operating conditions: 116 °C and 20 bar Kinetic model: LHHW Catalyst: Ni/Al_2O_3 Reaction mechanism: $CO + 3H_2 \leftrightarrow CH_4 + H_2O$	Zhang, et al. [69]

2.1.4. Boiler/turbogenerator

A substantial amount of energy is essential for various stages, including DA pretreatment, chemical hydrogenation, ethanol production, ethanol reforming, and CC unit. To meet this energy demand, solid residues, and tail gases from SC-1, as well as biogas and tail gas from SC-2, are combusted in a boiler to generate energy. The thermal energy required for SC-1 is supplied by a boiler plant, as depicted in Fig. 1, which is co-fired by lignin and tail gas produced from xylitol and ethanol reforming processes. Similarly, the thermal energy needed for SC-2, as seen in Fig. 2, is provided by burning biogas produced from biogas and tail gas from ethanol reforming. The utility conditions for both

scenarios are summarized in Table 2 and include low-pressure steam (LPS), HPS, and fired heat. The combustion of fuel is carried out with 20% excess air to generate superheated steam at 60 atm and 454°C, as well as fired heat at 850°C, to meet the heat requirement for the ethanol reformer. The high-pressure steam undergoes expansion through a turbine at 260°C and 13 atm to fulfil the steam requirement. This steam is divided into three different streams to meet the plant's steam demands: for DA pretreatment, to be mixed with ethanol in SRE, and to preheat the boiler feed water to 177°C. The steam requirement varies between SC-1 and SC-2 depending on the processes involved. The electricity is generated through the expansion of HP steam in the turbine. For units such as heaters, evaporators, and distillation in SC-1 and SC-2, LPS is required. However, since the combustion of fuel gas in the boiler is not enough to produce LPS, an external heat supply is necessary for the heating system [70].

Table 2. Fuel gas combustion and steam condition produced.

Parameter	Value	Ref
Boiler feed water pressure	62.2 atm	
Boiler feed water temperature	177 ^{o}C	
HP steam	62.2 atm	
HP steam temperature	452 ^{o}C	
Averaged burner temperature	870 ^{o}C	Humbird, et al. [55], Morakile, et al. [58], Özüdoğru, et al. [59]
LP steam	4.42 atm	
LP steam pressure	164 ^{o}C	
Fired heat temperature	850 ^{o}C	
Combustion conversion for solid part	98%	
Comp. isentropic/mechanical efficiency	89%/98%	
Turbine isentropic/mechanical efficiency	91%/98%	Zohrabian, et al. [71]

2.1.5. CC unit

The CC unit operates similarly in both SC-1 and SC-2, where the flue gas released from combustion undergoes treatment for CO_2 capture. Operating conditions, solvent composition, and process simulation validation data are sourced from the study by Hosseini-Ardali, et al. [72]. In this process, the flue gas from the boiler is directed to the CC unit and cooled to 40°C to enhance absorption in the absorber at atmospheric pressure. The flue gas enters the bottom of the absorber, while the solvent, composed of aqueous methyl-diethanolamine (MDEA, 18.5% w/w) and piperazine (PZ, 21.5% w/w), is introduced from the top in a counter-current flow. This solvent combination offers high degradation resistance, extending the solvent lifetime [73]. At the top of the absorber, the treated gas is drawn out, while a CO_2-rich amine solution is obtained at the bottom. This rich amine solution is pressurized to 2 bar and heated using the bottom stream of the stripper. To reduce the thermal energy required for solvent regeneration in the CO_2 stripper's reboiler, the CO_2-rich MDEA/PZ solution is pre-heated before entering the stripper. This pre-heating is accomplished by recovering heat from the hot CO_2-lean amine solution exiting the reboiler, with both streams flowing counter-currently [74]. In the stripper, the feed stream enters from the top, and the rich amine solution contacts the vapor phase produced in the counter-current flow mode with the reboiler, releasing absorbed CO_2 and solvent. The resulting CO_2 product, with a purity of 99 mol%, is obtained from the top of the tower. On the other hand, the lean amine solvent at the bottom of the distillation column is cooled by exchanging heat with the bottom stream of the flash drum. Then, the regenerated amine solvent is recycled back to the top of the absorber column.

2.1.6. Heat integration

In order to optimize the minimum utility requirement and its impact on the cost of utility and equipment installation, pinch analysis is employed for energy integration in H_2 production for both SC-1 and SC-2. This analysis is conducted using the Aspen Energy Analyzer, which allows for the evaluation of the Heat Exchanger Network (HEN) design and its effects on heating and cooling objectives, as well

as overall performance costs. The detailed HEN configuration and composite curve are provided in the supporting information. In this study, a minimum temperature difference of 10°C is used to achieve maximum energy recovery of cold and hot streams in all processes involved in both scenarios. Total cost, comprising energy utility cost and heat exchanger cost, is calculated to determine the economic feasibility of the proposed designs. The investment cost is computed by considering the required area and the minimum number of heat exchangers needed for the optimal operation of the system [75].

2.2. Process economics

Several economic parameters used to estimate investment and operating costs, as well as economic analysis are taken from [55, 76, 77], are summarized in Table 3 . The model biorefinery for H_2 production from both SCB and BW is assumed to be operated for 30-year plant life, based on similar steam reforming technologies [40]. The construction period is estimated to finish within 3 years, and the MARS method is adopted for depreciation estimation with 10 years of depreciation time. The total capital investment (TCI) of H_2 production from SCB and BW is estimated based on the total plant direct cost (TPDC), total plant indirect cost (TPIC), fixed capital investment, working capital, and land use. The equipment sizing is done according to the mass and energy balance data from the Aspen Plus model. The purchased equipment cost (TPEC) involved in this study is determined by Aspen Plus economic analyser for equipment, such as pump, compressor, turbine, heater, cooler, and distillation column. The other equipment purchase cost data are obtained from previous studies, including reactor and fermenter [51, 53, 55, 63, 78, 79], activated carbon tank and ion exchange tank [61], boiler [55], and PSA [71]. The equipment purchased cost was calculated by using the capacity and cost data of the benchmark system in the literature, as shown in Eq. (3).

$$new\ cost = \text{base cost} \times \left(\frac{\text{new size}}{\text{base size}}\right)^{\theta} \quad (3)$$

The new cost of the equipment was calculated from the base cost of the respective equipment with the known capacity. Where base size, new size, and θ are the capacity of the benchmark

equipment, current capacity, and scaling factor. The TPEC is then multiplied by the cost factors to obtain the TPDC, TPIC, and FCI, as shown in Table 3. In addition to capital investment, the annual operation cost encompasses the direct, fixed, and general manufacturing costs, as outlined in Table 3. The selection of raw material costs, utility costs, and product selling price is crucial for the economic evaluation of the project, as it significantly influences the outcomes of the analysis. Information regarding catalyst requirements is obtained from the works of Sladkovskiy, et al. [51] for APR and Compagnoni, et al. [40] for SRE. Catalysts are considered in the capital expenditure (CAPEX) and not in the operational expenditure (OPEX), and the reactors are assumed to undergo catalyst replacement every five years [40, 80]. Furthermore, the revenues generated by the process are estimated based on the main product and co-products, which include H_2, gypsum, fertilizer, and electricity, as detailed in Table 4. The total annual revenue is calculated by summing the unit prices of the products and by-products multiplied by their production rates. The selling price of H_2 is a critical parameter for estimating revenue. Therefore, it is assumed that the price used reflects the price of H_2 fuel [53, 81]. A higher selling price would enhance the economic competitiveness of the process.

Table 3. Economic evaluation parameters for H_2 production systems.

Parameter	Value/comment
Plant location	United Kingdom
Plant operation and life	8000 hours and 30 years
Discount rate	10%
Federal tax rate	25% (the UK case)
Financing	100% equity

Construction period	3 years
First 12 months' expenditures	8%
Next 12 months' expenditures	60%
Last 12 month's expenditures	32%
Depreciation method	MARS
Depreciation time	10 years
TCI	TCI = FCI + working capital + land use
Total plant direct cost (TPDC)	$TPDC = C_{EC} + C_{EI} + C_{ICS} + C_{Pp} + C_{Ee} + C_B + C_S + C_{AF}$
Equipment cost (C_{EC})	All equipment costs involved in the process
Equipment installation (C_{EI})	39% of C_{EC}
Instrumentation and control system (C_{ICS})	13% of C_{EC}
Process piping (C_{Pp})	31% of C_{EC}
Electrical equipment (C_{Ee})	10% of C_{EC}
Buildings (C_B)	29% of C_{EC}
Site development (C_S)	10% of C_{EC}
Auxiliary facilities (C_{AF})	55% of C_{EC}
Total plant indirect cost, (TPIC)	TPIC = Ceng + Ccon
Engineering (C_{Eng})	32% of C_{EC}
Construction (C_{Con})	34% of C_{EC}
Total plant cost (TPC)	TPC = TPDC + TPIC
Contractor's fee (C_{Cf})	5% of TPC
Contingency (C_C)	10% of TPC
Fixed capital investment (FCI)	$FCI = TPC + C_{Cf} + C_C$
Working capital	10% of FCI
Land use	5% of EC

TCI	TCI = FCI + working capital + land use
Direct manufacturing cost (DMC)	
Raw materials cost (C_{RM})	All raw material cost requirements
Utilities cost (C_{UT})	All utilities cost requirements
Operating labor (C_{OL})	Cost of plant employees
Supervisory and clerical labor	20% of C_{OL}
Maintenance and repair	6% of FCI
Operating supplies	0.9% of FCI
Laboratory charges	15% of C_{OL}
Patents and royalties	3% of COM ($COM = 0{,}28\ FCI + 2{,}73\ C_{OL} + 1{,}23\ (C_{UT} + C_{WT} + C_{RM})$)
Fixed manufacturing cost (FMC)	
Local taxes and insurance	3% FCI
Plant overhead	70.8% of C_{OL} + 3.6% FCI
General manufacturing cost (GMC)	
Administration costs	17.7% of C_{OL} + 0.9% FCI
Distribution and selling costs	11% of COM
Research and development	5% of COM
Annual operating expenditures	Annual OPEX = DMC + FMC + GMC

Table 4. Raw material cost, utilities cost and selling prices of product.

Parameter	Unit cost	Price	Ref
Raw material			
SCB	$/MT	50	Gadkari, et al. [23]
BW	$/MT	100	Mailaram, et al. [79]
Sulfuric acid	$/kg	0.07	Gadkari, et al. [23]

Enzyme	$/kg	2.65	Banerjee, et al. [82]
Yeast extract	$/kg	0.0052	Chong, et al. [66]
Peptone	$/kg	0.0052	Chong, et al. [66]
Ammonium sulphate	$/kg	0.1	Regis, et al. [83]
Magnesium sulphate	$/kg	0.18	Regis, et al. [83]
Potassium phosphate	$/kg	1.2	Regis, et al. [83]
Process water	$/1000 L	0.177	Thanahiranya, et al. [84]
Catalyst			
Nickel	$/kg	24.5	Yan, et al. [54]
Iron	$/kg	0.31	Wee, et al. [53]
Copper	$/kg	5.83	Wee, et al. [53]
Pt	$/kg	25	Sladkovskiy, et al. [51]
Utilities			
Cooling water	$/L	0.032	Mailaram, et al. [79]
Electricity	$/kWh	0.77	Gadkari, et al. [23]
Low pressure steam	$/kg	0.018	Mailaram, et al. [79]
Products			
Gypsum	$/MT	34.69	Wiranarongkorn, et al. [85]
CO_2	$/MT	120	Nouwe Edou and Onwudili [86]
Fertilizer	$/MT	19.6	Li, et al. [87]
H_2	$/kg	16.5	Wee, et al. [53], Melikoglu and Tekin [81]

The economic analysis focuses on assessing the project's feasibility through various financial metrics: profit, NPV, IRR, PBP, H_2 production cost, and LCOH. Gross profit is calculated as the difference between revenue and all operational expenses. NPV measures the difference between the present value of cash inflows and outflows. It is used in capital budgeting to analyse the profitability of a

projected investment or project. NPV is used to determine the profitability of a project, which is calculated between the present value of cash inflows and outflows over a period of time. Where *i* is the discount rate (10%), n is the lifetime of the plant (30 years), and TCI is the total capital investment. NPV is the sum of a project's discounted net cash flows over its lifespan, evaluated using the industry's benchmark rate of return to reflect profitability throughout the entire project, as shown in Eq. (4).

$$NPV = -TCI + \sum_{t=1}^{n} \frac{\text{Net cash flow}}{(1+r)^{i}} \tag{4}$$

IRR is a metric used in capital budgeting to measure the profitability of potential investments. It is a discount rate that makes the NPV of all cash flows from a particular project equal to zero. The IRR is the discount rate that sets the NPV equal to zero and can be calculated by Eq. (5).

$$0 = -TCI + \sum_{t=1}^{n} \frac{\text{Net cash flow}}{(1+\text{IRR})^{t}} \tag{5}$$

Furthermore, PBP is the TCI divided by annual net profit. It refers to the time required to repay the initial investment with income from the beginning of the project, which can be calculated from Eq. (6).

$$PBP = \frac{\text{Total capital investment}}{\text{Annual net profit}} \tag{6}$$

The unit H_2 production cost is obtained from the total annual costs and the annual H_2 production using Eq. (7).

$$Unit\ H_2\ production\ cost\ \left(\frac{\$}{kg\ H_2}\right) = \frac{\text{Total annual costs}\ \left(\frac{\$}{y}\right)}{\text{Annual H}_2\ \text{production}\ \left(kg\frac{H_2}{y}\right)} \tag{7}$$

The LCOH can be calculated as the ratio of the total lifetime costs (CAPEX and OPEX) to the total lifetime H_2 production, as shown in Eq. (8).

$$LCOH\left(\frac{\$}{kg\ H_2}\right) = \frac{\text{Total lifetime costs (Capex + Opex)}}{\text{Total lifetime H}_2\ \text{production}} \tag{8}$$

3. Results and discussion

3.1. Mass and energy balance

Table 5 provides a comprehensive overview of the mass and energy balances associated with H_2 production from SCB and BW. Notably, the total H_2 produced from SCB in SC-1 (159.88 kg/hr) was lower than that from SC-2 (199.40 kg/hr) due to the lower ethanol yield in SC-1 (564.71 kg/hr). In comparison, SC-2 resulted in almost twice the amount of ethanol (1,034.70 kg/hr), as higher ethanol consumption led to higher H_2 generation. Generally, the H_2 yield from the SRE process was approximately 19% in both scenarios, aligning with the findings of Compagnoni, et al. [40], who produced 889 kg/hr of H_2 from 4,567 kg/hr of ethanol. Additionally, the additional H_2 yield from xylitol in SC-1 was relatively modest at 6%, consistent with the findings of Murzin, et al. [48]. It is worth mentioning that the H_2 yield based on the feedstock was 38.37 g H_2/ kg SCB and 47.86 g H_2/kg BW. These yields were notably lower compared to alternative processes, such as woody biomass gasification, which produced 87 g H_2/kg Biomass [88] and food waste torrefaction, achieving 129.4 g H_2/kg Biomass [89]. Thermochemical processes achieve higher H_2 yields by operating at significantly higher temperatures, which promote a greater degree of thermal cracking [90]. This elevated heat facilitates the efficient conversion of feedstock into syngas, allowing for the complete utilization of organic materials, such as cellulose, hemicellulose, and lignin, and ultimately resulting in higher hydrogen production [91]. While the H_2 yields demonstrate the potential efficiency of SCB and BW, the economic viability of these systems also benefits from the valuable by-products produced. The by-products generated varied between the two scenarios between SC-1 and SC-2, with gypsum produced at approximately 104.95 kg/hr from the neutralization process of hydrolysate and fertilizer obtained from biogas production in the AD process, accounting for 198.082 kg/hr. These by-products offer potential revenue generation for the plant [92, 93].

Energy generation involves the recovery of solid residues and tail gas for SC-1 and biogas and tail gas for SC-2. SC-1 yielded significant solid residues (1,000.911 kg/hr) from solid-liquid separation in ethanol production, containing more lignin mixed with unconverted hemicellulose and cellulose

during DA pretreatment. The tail gas produced from the reforming of xylitol and ethanol, generated at a rate of 1,984.83 kg/h, contains a high concentration of hydrogen (42.82 mol%) along with small amounts of methane (1.24 mol%) and alkanes (C1-C5), each comprising less than 2 mol%. This gas was utilized as a fuel in the boiler. The combustion of both streams produced 7.36 MW of thermal energy, of which 1.89 MW was allocated for heating the heater and the SRE reactor. The remaining 5.47 MW was used to generate HP steam at 454°C and 60 atm, producing approximately 7,831.92 kg/h of HP steam. This steam was then divided into two streams: the first (5,208.23 kg/h) was directed to the APR reactor as a heating medium, while the second (2,623.69 kg/h) was expanded to 13 atm for electricity generation, yielding 0.282 MW of power. Additionally, another stream of HP steam, generated at 260°C and 13 atm, was further divided. One portion, amounting to 1,834.577 kg/h, was used to meet the HP steam demand for DA pretreatment. The remaining portion was expanded to 1 atm, generating an extra 0.092 MW of electricity. In total, the electricity generation in SC-1 reached 0.374 MW, more than sufficient to cover the total electrical consumption of 0.142 MW, with an excess of 0.232 MW available for sale to the grid. However, the LP steam required for other units, including the heater, distillation column, stripper, and evaporator, had to be supplied externally, amounting to 16,175.17 kg/h.

In comparison, SC-2 generated less thermal energy from the burned fuel gases (biogas and tail gas) because the tail gas and biogas had high CO_2 contents of 59.2% mol and 31% mol, respectively, resulting in a lower HHV. Combusting biogas and tail gas produced 3.92 MW of thermal energy, out of which 2.78 MW utilized for heating the SRE reactor and the remainder for generating HP steam. The steam produced (2,107 kg/hr) was expanded to 13 atm, generating electricity (0.206 MW). Similarly, the generated electricity was adequate to fulfil all electrical demands (0.023 MW), with the surplus being sold to the grid at 0.183 MW. The steam expanded was divided into two streams for different purposes: one stream was utilized for preheating the feedwater boiler (349.15 kg/hr), and the second stream (1757.85kg/hr) was utilized for heating before autoclave. However, the final stream expanded

to LP steam was insufficient to meet the LP steam requirements. Consequently, all LP steam requirements, totalling 8772.27 kg/hr, would be externally supplied.

Table 5. Mass and energy balance performed in H_2 production for SC-1 and SC-2.

Parameter	Unit	SC-1	SC-2
Feedstock	MT/day	100	100
Xylitol produced (20 wt%)	kg/hr	2745.82	-
Ethanol produced (33.86 wt%)	kg/hr	1958.31	3055.59
H_2 produced from xylitol	kg/hr	33.88	-
H_2 produced from ethanol	kg/hr	126	199.40
H_2 consumed in hydrogenation	kg/hr	8.253	-
Net H_2 produced	kg/hr	151.62	199.40
Gypsum produced	kg/hr	104.95	-
Fertilizer produced	kg/hr	-	595.50
Fuel consumption			
Solid residues generated	kg/hr	1000.911	-
HHV of solid residues	MJ/kg	43.54	-
Total tail gas generated	kg/hr	1984.83	1883.89
Tail gas composition			
Water	Mol	0.38%	0.6%
H_2	Mol	42.82%	36.1%
CO_2	Mol	54.2%	59.2%
CH_4	Mol	1.24%	4.1%
C_3H_8	Mol	1.22%	-

C_2H_6	Mol	0.12%	-
C_4H_{10}	Mol	0.015%	-
C_5H_{12}	Mol	0.007%	-
HHV of tail gas	MJ/kg	6.39	5.08
Biogas produced	kg/hr	-	499.26
HHV of biogas	MJ/kg	-	16.43
Energy requirements			
Thermal energy produced	MW	7.36	3.92
Thermal energy consumption			
Fired heat	MW	1.89	2.78
Steam generation	MW	5.47	6.29
Electricity produced	MW	0.374	0.206
Electricity consumed	MW	0.142	0.023
Surplus electricity	MW	0.232	0.183
Carbon capture			
Flue gas	kg/hr	12657.1	7716.8
Treated gas	kg/hr	9280.629	5280.80
CO_2 captured	kg/hr	3682.61	2489.75
Rich loading	(mol CO_2/mol amine)	0.57	0.58
Specific reboiler duty	(GJ/t CO_2)	4.08	4.06

The flue gas of SC-1 exhibited a higher concentration compared to SC-2 due to increased fuel gas combustion; nonetheless, both scenarios resulted in a post-combustion CO_2 concentration of approximately 20% mol [94]. The treated gas released for SC-1 and SC-2 amounted to 12,657.1kg/hr and 7,716.8kg/hr, respectively. These gases primarily consisted of N_2 (~79%), with a minimal CO_2

concentration (< 1.5% mol). Additionally, SC-1 captured a higher total of CO_2 (3,682.61kg/hr) compared to SC-2 (2,489.75kg/hr).

3.2. Heat integration

In the current investigation, we employed heat integration through pinch analysis to enhance the energy utilization efficiency of the proposed integrated H_2 production system. Fig. 3 illustrates the heating and cooling consumption before and after the implementation of heat integration. Prior to heat integration, the total duty of heating and cooling for SC-1 stood at 19.94 MW and 22.85 MW, respectively. The primary contributor to heating consumption, at 4.53 MW, was the evaporation of water content to 20% of xylitol concentration before chemical hydrogenation. Another energy-intensive process was the heating duty of the reformer for both xylitol and ethanol, totalling 4.71 MW and 1.64 MW, respectively, necessitating high reaction temperatures for effective reaction. Additionally, the heating requirement in the reboiler of the CCU was substantial at 4.16 MW due to the release of CO_2 gas from the solvent mixture. To optimize energy use, a heat recovery strategy employing heat integration was implemented. The composite curve and detailed heat exchanger networks used for this optimization are provided in the supporting information. Heat recovery potential was notable, with 3.83 MW recovered from the DA, xylitol, and ethanol production areas, and an additional 4.58 MW recovered from the SRE and APR areas. Post-heat integration, a significant reduction in heating duty consumption, by 27%, was achieved post-heat integration. The extraction of energy from effluent reformers (APR and SRE) had a substantial impact on heating consumption, with impressive reductions of 38% and 28%, respectively, observed in reformers. Similarly, the highest cooling demand of SC-1 stemmed from the need to lower the combined stream of evaporator effluent in xylitol production, amounting to 4.42 MW, where a considerable amount of water generated with two-phase formation would be recycled back to the DA pretreatment. The reformers and CCU also required high cooling demand, with 5.87 MW and 7.56 MW, respectively. The cooling energy was

reduced by 45%, totalling 12.48 MW. The most notable reduction in cooling duty was observed in CCU at 70%, followed by reformers at 43% and 21% reduction in xylitol hydrogenation.

Before heat integration, the heating and cooling requirements of SC-2 were 17.75 MW and 26.41 MW, respectively. The most energy-intensive process was the pre-heating of BW slurry (20 wt%) before autoclaving, accounting for 7.28 MW. This was followed by the energy requirements of the reboiler in the CCU and heating in the SRE reactor, totalling around 2.81 MW and 4.07 MW, respectively. After heat integration, the potential heat recovery was estimated at 7.8 MW in the ethanol production area and 1.46 MW in the reforming area. As a result, heating and cooling demands were reduced by approximately 49% and 33%, respectively. The greatest energy-saving potential was observed in the effluent stream of the autoclave, where heat exchange with the cooled BW slurry stream led to a reduction of 86% in heating demand and 39% in cooling demand. Similarly, heat and cooling exchanges in the feed preheating and effluent streams of the SRE reactor contributed to a 32% reduction in heating demand and a 57% reduction in cooling demand. Additionally, energy recovery from the bottom stream of the reboiler in the CCU and the effluent of the absorber resulted in a 15% reduction in both heating and cooling demands.

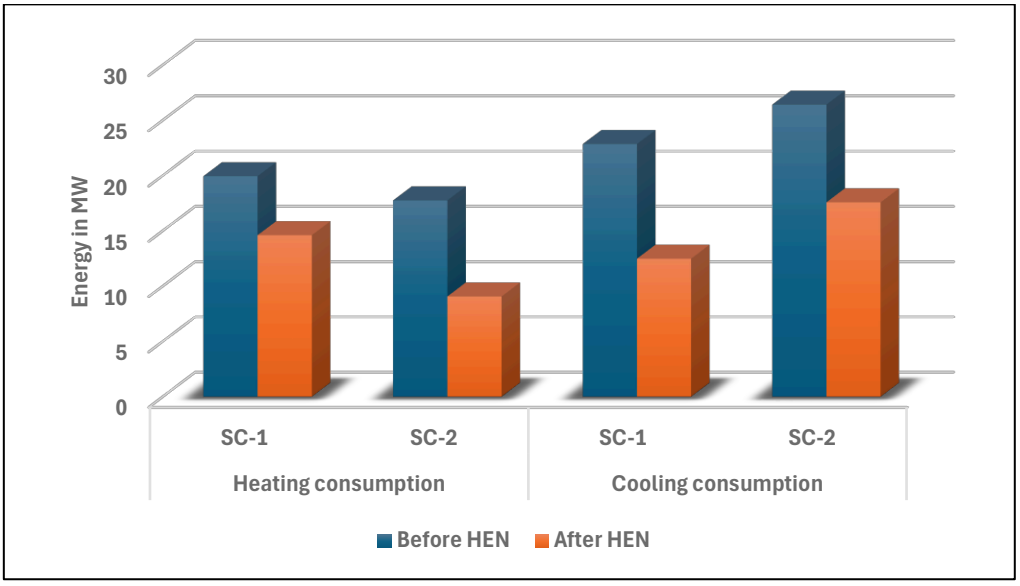


Fig. 3. Energy (heating and cooling) requirements before and after integration.

3.3. Economic feasibility

The economic evaluation of H_2 production from SCB and BW is outlined in Table 6. It was evident that the investment required for H_2 production in SC-1 exceeded that of SC-2, with estimates of 68.3 and 49.8 M$ respectively. This higher investment in SC-1 could be attributed to the pretreatment of SCB and the chemical hydrogenation processes involved, which incurred additional costs. Additionally, the H_2 production from xylitol reforming added to the investment in SC-1. These three additional processes collectively contributed to a 44.55% increase in the investment for SC-1. Conversely, SC-2 involved fewer processes for H_2 production, primarily relying on the conversion of carbohydrates contained in BW to ethanol, which was subsequently transformed into H_2. Notably, ethanol production accounted for the highest capital expenditure in both SC-1 and SC-2, with over 3 M$ of the total equipment cost. This was followed by the hydrogen reforming processes, which accounted for approximately 33.1 M$ in SC-1 and 23 M$ in SC-2.

Table 6. Capital investment, production cost and profitability analysis for H_2 production.

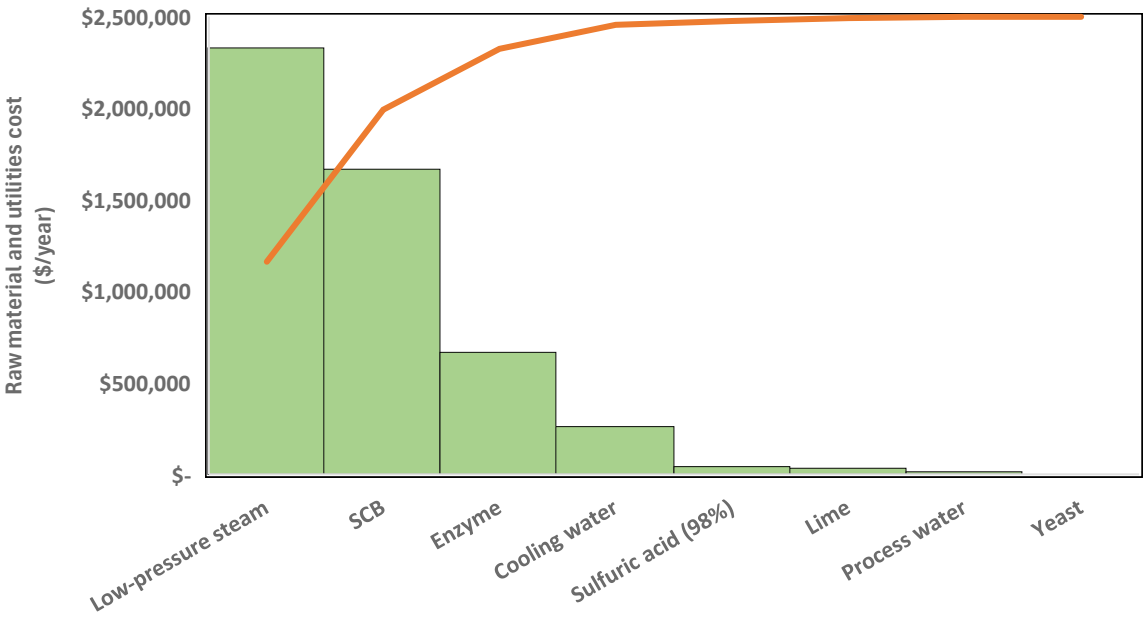
Economic parameters	**SC-1**	**SC-2**
Dilute acid pretreatment	$2,412,919	-
Xylitol production	$2,778,008	-
Ethanol production	$3,293,586	$3,391,886
Anaerobic digestion	-	$2,042,000
Xylitol reforming	$1,419,465	-
Ethanol reforming	$1,633,787	$2,290,896
Boiler	$2,497,580	$2,491,564
CCU	$487,700	$440,100
Catalyst	$315,675	$356,524

TPEC	**$14,838,718**	**$11,012,970**
Capital expenditure		
TPDC	$43,327,548	$31,607,223
TPIC	$9,963,826	$7,268,560
TPC	$53,291,374	$38,875,783
FCI	$61,285,081	$44,707,151
Land use	$905,802	$660,778
Working capital	$6,128,508	$4,470,715
TCI	**$68,319,391**	**$49,838,644**
Operational expenditure		
DMC	$14,533,893	$11,166,849
FMC	$4,986,732	$3,892,588
GMC	$4,823,315	$3,685,105
OPEX	**$24,343,940**	**$18,744,542**
Revenues		
H_2	$21,103,851	$26,320,843
Gypsum	$28,916	-
Fertilizer	-	$93,374
Electricity	$142,961	$112,763
CO_2	$4,143,952	$3,339,073
Total	**$25,419,681**	**$29,866,053**
Profitability analysis		
H_2 Production cost ($/kg H_2)	17.20	11.75
NPV ($)	-63,673,649	36,449,937
IRR (%)	-5	17

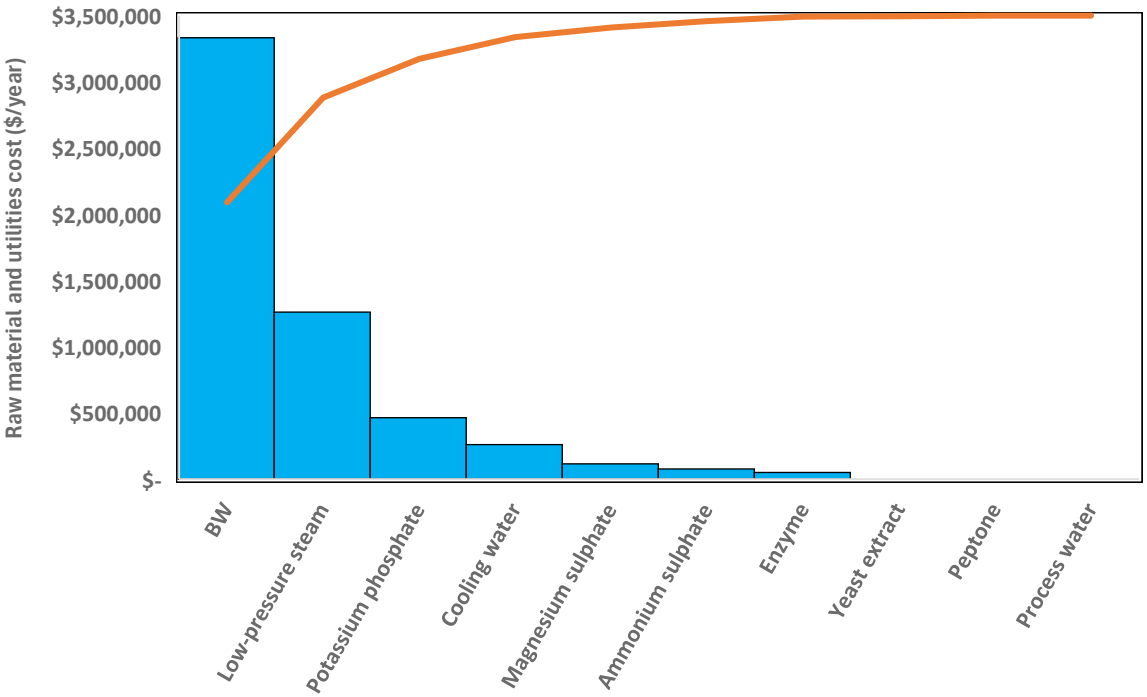
PBP (years)	35	11
LCOH ($/kg H_2)	20.81	12.97

The total operating cost of SC-1 amounted to 24.3 M$/year, representing a 15% increase compared to SC-2, which stood at 18.7 M$/year. Dominated by the DMC, which accounted for 60%, and followed by the FMC at 21%, the operating costs were primarily driven by raw materials and utilities consumption within the DCM. The Pareto graph depicted in Fig. 4a and 4b elucidated the contribution of each raw material and utility consumed in both SC-1 and SC-2. The cost analysis revealed that the most significant expense in H_2 production for the SC-1 was attributed to LPS requirements, amounting to 2.3 M$/year, followed by SCB feedstock costs, which accounted for 1.7 M$/year. Whereas, the SC-2 incurred even higher feedstock cost, with BW accounting for 3.3 M$/year, in addition to 1.3 M$/year for LP steam. Recent studies have estimated the cost of biomass used in H_2 production to range between 60 and 100 $/tonne [95-98]. Wu, et al. [99] further highlighted that biomass feedstock costs contribute significantly, comprising approximately 30% of the total production cost. It is noteworthy that the elevated feedstock costs for both SCB and BW considered the collection and transportation expenses of the feedstock to the H_2 plant location [23, 79]. The reduction in both the cost of feedstock (SCB and BW) and LP steam significantly enhances the profitability of H_2 production from SCB and BW. Additionally, another significant cost factor was LP steam, reflecting the high energy requirements for downstream processes in xylitol and CCU for SC-1, and ethanol and CCU for SC-2. The makeup cost of H_2 for chemical hydrogenation and electricity consumption in the overall process had no bearing on H_2 production costs, as these materials were all supplied by the H_2 produced in reforming and electrical generation in the turbogenerator. The enzyme costs for SC-1 and SC-2 showed a significant difference in their contribution to the total raw material expenses. Specifically, enzymes accounted for 28% of the raw material cost in SC-1, compared to just 1% in SC-2. This notable discrepancy arises from the difference in enzyme usage between the two systems: SC-1 required 7.5 mg/ g SCB [100] , whereas SC-2 used only 0.6 mg/g BW [31]. The reliance on lignocellulosic biomass in SC-1 necessitated higher

enzyme quantities, as highlighted by Gadkari, et al. [23], who noted that the cost of enzymes for converting cellulose to glucose is a major contributor to the overall raw material cost. Similarly, Qian, et al. [101] supported this observation, emphasizing that reducing enzyme costs is a key factor in achieving economic feasibility for such processes.



(a)



(b)

Fig. 4. Contribution of the individual raw materials and utilities cost: (a) SC-1; (b) SC-2.

To assess the economic viability of the proposed processes, various criteria, such as the profitability index, H_2 production cost, NPV, IRR, PBP and LCOH are utilized. Revenue streams included the selling prices of both the main product and co-products. SC-1's total revenue was comprised of sales from H_2 (21 M$/year), gypsum (0.028 M$/year), electricity (0.14 M$/year), and CO_2 (4.1 M$/year). However, SC-2, which produced H_2 from BW, demonstrated higher revenues at 29.86 M$/year compared to SC-1's 25.42 M$/year. This disparity was mainly due to the higher selling price of H_2 and the increased H_2 yield from BW, contributing over 88% to the revenues. The CO_2 captured contributed slightly to the revenues, accounting for 11% or 3.3 M$/year. In SC-2, fertilizer production made a minor contribution of less than 1%. The production cost of H_2 from BW was notably lower than that from SCB, at 12.93 $/kg H_2 and 17.20 $/kg H_2, respectively. The lower annual operating cost and higher H_2 yield in SC-2 were the primary factors leading to its lower production cost. Examining the economic parameters provided in Table 6, the financial performance of the analysed H_2 production systems was evaluated across different strategies. Notably, the NPV for the SC-2 system was positive, reaching 36.45 M$, highlighting the financial viability of H_2 production through BW valorization. SC-2, in particular, proved to be the more profitable system for hydrogen production, with a PBP of 11 years and an IRR of 17%. Additionally, SC-2 demonstrated a significantly lower LCOH of 12.97 $/kg compared to 20.81 $/kg for the SC-1. These figures suggest a high potential for financial returns and underscore the economic attractiveness of SC-2. This success was primarily attributed to substantial H_2 profits and lower investment and annual operating costs. In contrast, the NPV value for systems operating under SC-1 was negative, signifying that H_2 production from SCB was not economically attractive. The primary obstacle lay in their lower revenue generation, which significantly impacted their economic performance unfavourably.

Table. 7. Summary of profitability analysis of H_2 production from various feedstock and processes.

Feedstock	Processes	Production cost ($/kg)	NPV (M$)	IRR (%)	PBP (years)	LCOH ($/kg)	Ref
Lignocellulosic biomass resources							
MSW	gasification	-	42.78	10.3*	9	2.72	Ren, et al. [102]
POME	SRM	12.9	-	18.5*	8.5	-	Wee, et al. [53]
Sorbitol	APR	12.97	-	-	-	-	Sladkovskiy, et al. [51]
Pine wood	FB gasification	4.3	-	-	-	-	Salkuyeh, et al. [98]
Glycerol	SCWR	3.8	-	-	7.5		Galera and Gutiérrez Ortiz [5]
SCB	APR and SRE	17.20	-63.67	-5	-	20.81	This study
Water resources							
Water	Electrolysis	-	-	-	6.9	5.84	Yilmaz, et al. [103], Parkinson, et al. [104]
Water	PEM electrolysis	-	9.09	12.8	13	4.21	Pettinau, et al. [105]
Food waste resources							
FW	TG	1.33	19.8	25	5.7	-	Zhao, et al. [89]
FW	DG	1.42	13.7	20.4	7.2	-	Zhao, et al. [89]
BW	Fermentation	14.89	1.2	-	4.8	-	Han, et al. [106]
BW	SRE	11.75	36.45	17	11	12.97	This study

FB: Fluidized bed, FW: Food waste; MSW: municipal solid waste; PEM: proton exchange membrane; TG: Torrefaction integrated with steam gasification; DG: Direct gasification; SRM: Steam methane reforming; POME: palm oil mill effluent; SCWR: Supercritical water reforming; *calculated by return on investment (ROI).

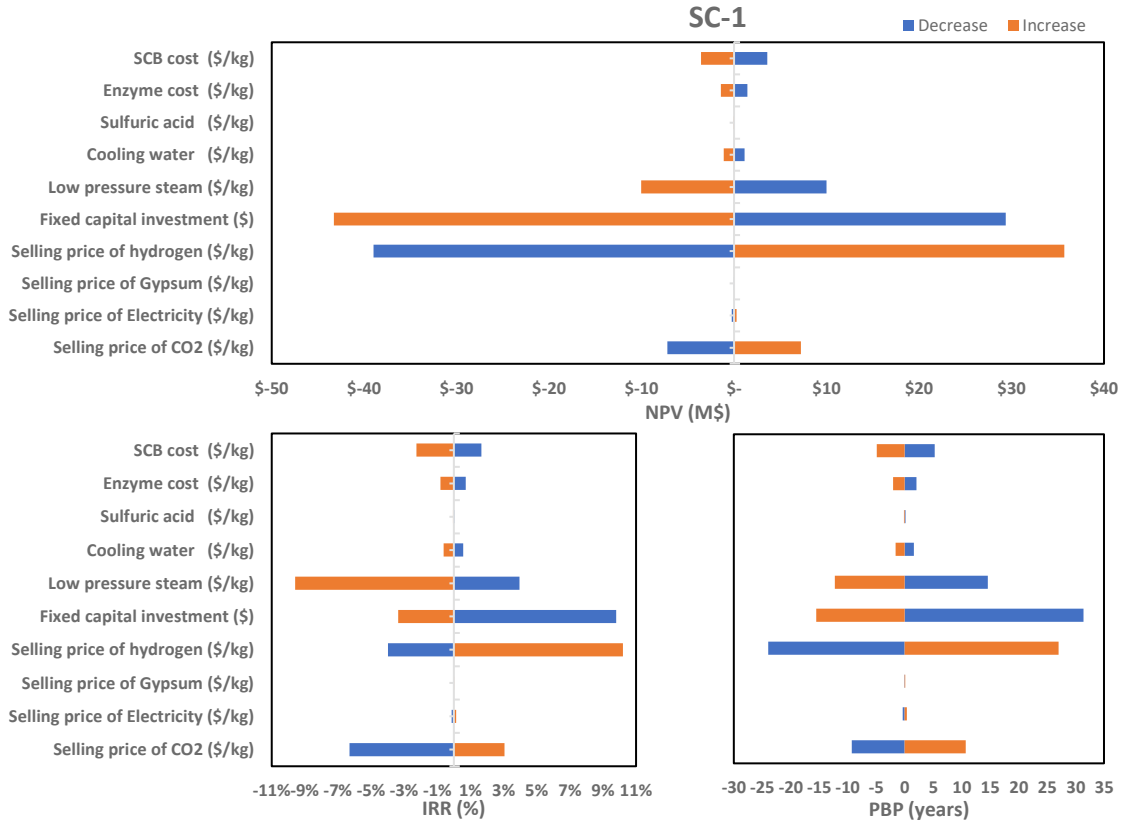
The profitability analysis summary from various feedstocks and H_2 production processes is listed in Table 7. However, the production cost of H_2 varies depending on factors such as feedstock price, facility scale, and project economics [104]. Exploration of alternative processes for H_2 production from non-fossil resources proved intriguing Zhao, et al. [89] demonstrated FW-based H_2 production with a production cost below 1.5 $/kg H_2, short PBP (5.7 years), high IRR (25%), and NPV (19.8 M$). This was attributed to lower annual operating costs and total production expenditure, with significant contributions from government subsidies and disregarding collection and transportation expenses of FW feedstock. POME, generated from palm oil mill activities, was another viable feedstock. Wee, et al. [53] illustrated profitable H_2 production from POME with a PBP of 8.5 years and an 18.48% of ROI, based on a feedstock capacity of 480 MT/day. This process involved producing H_2 from biogas generated through AD, followed by steam methane reforming. Lower investment and production costs were incurred compared to other processes. H_2 production from BW performed by Han, et al. [106] via fermentation in CSTR tanks proved profitable at small capacities of 2 MT/day. However, production costs were high due to significant utility (electricity and process water) and labour costs. Nonetheless, the few by-products produced (CO_2, solid biomass, and treated BW) contributed substantially to revenue. The profitability analysis showcased the attractiveness of the plant, with an NPV of 1.2 M$ and a PBP of 4.8 years. A strategic approach is necessary to enhance the economic competitiveness of waste-based feedstocks in large-scale H_2 production applications [107]. Despite challenges, the studies presented above highlight the significant potential for H_2 production from non-fossil resources, offering promise and sustainability for the future by utilizing renewable substrates [106].

3.4. Sensitivity analysis

To address the uncertainty surrounding the cost-effectiveness O_2 production processes, sensitivity analysis was conducted to evaluate how variations in input parameters affect model outputs. Fig. 5 (a-b) illustrates the sensitivity analysis for both scenarios, examining the NPV, IRR, and PBP response to ±20% changes in key factors. The cost of raw materials, specifically SCB and BW, along with utilities like LPS and FCI, emerged as primary determinants of economic performance. The selling prices of H_2 product and CO_2 co-product also significantly impacted the NPV, IRR, and PBP. Conversely, costs for cooling water and enzymes exhibited minimal sensitivity to NPV, IRR, and PBP under the evaluated conditions.

In the SCB-based H_2 production scenario (SC-1), a key factor was the SCB cost, where a 20% reduction increased the NPV by 3.58 M$. LPS costs showed a notable impact, with a 20% reduction resulting in an increase in NPV by 10.01 M$. The most critical investment cost was FCI, where reductions could decrease NPV by 43.28 M$, while the H_2 selling price had the most substantial effect, with a 20% increase boosting NPV by 39 M$. Both parameters were also significant for IRR and PBP. Reducing FCI by 20% would remarkably improve the IRR by 9.79% and lower the PBP by 15 years. Similarly, increasing the H_2 selling price by 20% would enhance the IRR by 10.2% and lower the PBP by 27 years. Insignificant factors included sulfuric acid costs and cooling water, where 20% reductions only slightly improved NPV. Gypsum and electricity prices had minimal impact, raising NPV by less than 1 M$ each with a 20% increment. In the BW-based H_2 production scenario (SC-2), the BW cost was highly significant, with a 20% decrease increasing NPV by 6.2 M$. LPS costs also showed a substantial impact, with a 20% increase reducing NPV by 4.7 M$. The FCI reduction significantly improved NPV by 45.74 M$, while the H_2 selling price had the most significant effect, with a 20% increase raising NPV by 41 M$. These parameters also significantly affected IRR and PBP. Lowering FCI by 20% increased IRR by 6% and shortened PBP by 9 years. Similarly, raising the H_2 selling price by 20% increased IRR by 9.1% and reduced PBP by 17 years. Insignificant factors included enzyme and potassium costs, where 20% increases resulted in less than a 1 M$ NPV reduction each, and cooling water costs, which had less impact compared to LPS.

To enhance the profitability of H_2 production processes from SCB and BW, several strategic measures can be adopted. Lowering FCI is critical, and can be achieved through optimizing plant design, leveraging government incentives, and scaling up production to benefit from economies of scale. Reducing LPS costs is also essential, which can be done by improving energy efficiency. Additionally, optimizing raw material costs by strategically sourcing SCB and BW from nearby suppliers can significantly reduce transportation and logistics expenses. These measures, combined with supportive policies and efficient cost management, are crucial for improving the economic feasibility and profitability of H_2 production from SCB and BW feedstocks.



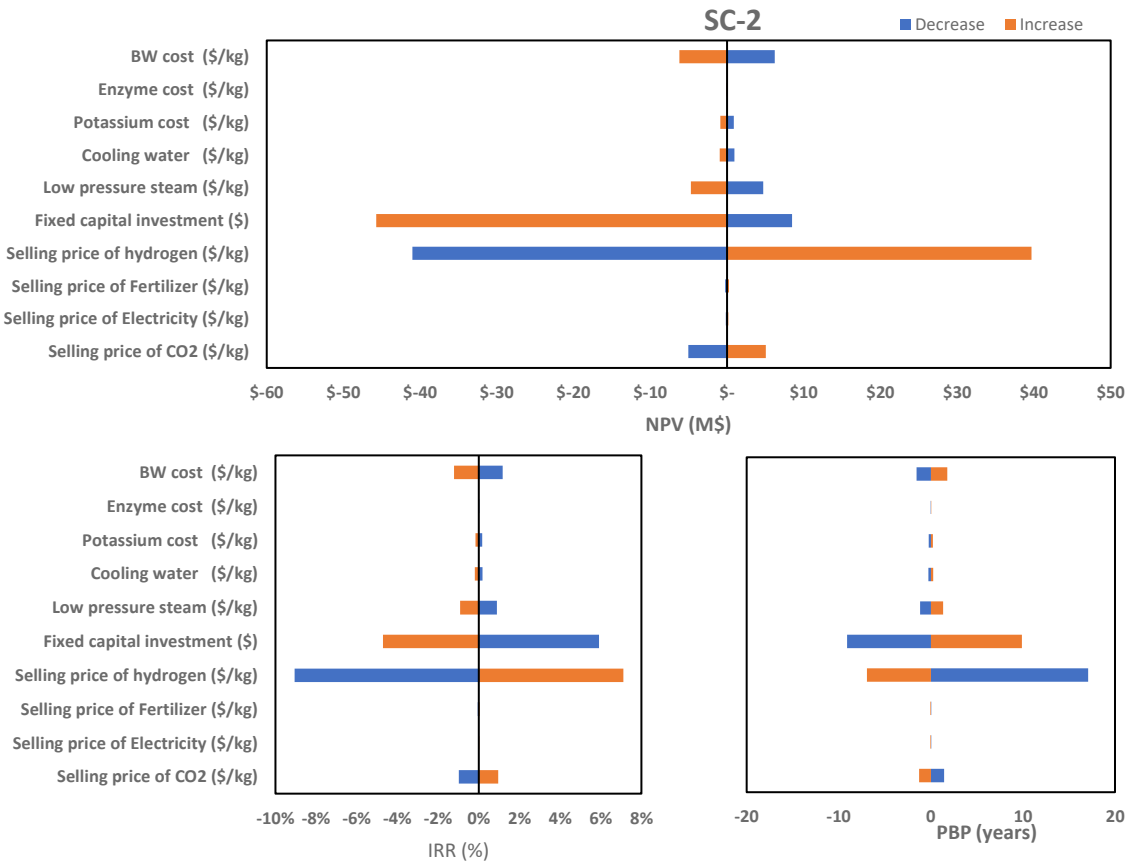


Fig. 5. Sensitivity analysis for different scenarios: (a) SC-1; (b) SC-2.

4. Conclusion

This study investigates the economic profitability of H_2 production from two alternative feedstocks: SCB and BW. The results reveal that the total H_2 produced in the SCB-based scenario (SC-1) is higher compared to the BW-based scenario (SC-2), primarily due to the increased bioethanol production. However, SC-1 demonstrates higher energy generation because of the higher fuel consumption and the greater HHV of the fuel burned. Economically, SC-2 emerged as the more attractive process, with a higher NPV of 36.45 M$, an IRR of 17%, and a PBP of 11 years. This economic attractiveness is attributed to lower capital investment and annual operational costs, which lead to higher profitability in the BW-based H_2 process. To enhance profitability, optimize plant design, use government incentives, and scale up production to reduce FCI. Lowering LPS costs can be achieved by improving energy efficiency. Source SCB and BW locally to reduce transportation expenses. These strategies,

supported by efficient cost management and policies, are essential for making H_2 production from SCB and BW economically viable. Future work should focus on conducting a comprehensive Life Cycle Assessment (LCA) to evaluate the environmental impacts of using these renewable feedstocks for H_2 production. This will help determine whether both SCB and BW are environmentally attractive options for sustainable H_2 production.

Acknowledgements

Dr. Gadkari would like to acknowledge the financial support from the Natural Environment Research Council (NERC) UK project grant: NE/W003627/1.

CRediT authorship contribution statement

Rendra Hakim Hafyan: Methodology, Resources, Formal analysis, Data curation, Visualization, writing – original draft, writing – review & editing. **Vinod Kumar**: Conceptualisation, Writing – review & editing. **Sunil K. Maity:** Writing – review & editing. **Jhuma Sadhukhan:** Methodology, Writing – review & editing. **Siddharth Gadkari:** Funding acquisition, Methodology, Resources, Formal analysis, Data curation, Supervision, Visualization, writing – review & editing. All authors read and approved the final manuscript.

Declaration of competing interest

The authors declare that they have no known competing financial interests or personal relationships that could have appeared to influence the work reported in this paper.

Reference

[1] Q. Hassan *et al.*, "The renewable energy role in the global energy Transformations," *Renewable Energy Focus,* vol. 48, p. 100545, 2024/03/01/ 2024, doi: https://doi.org/10.1016/j.ref.2024.100545.

[2] P. Lakhtaria, P. Ribeirinha, W. Huhtinen, S. Viik, J. Sousa, and A. Mendes, "Hydrogen production via aqueous-phase reforming for high-temperature proton exchange membrane fuel cells-a review," *Open Research Europe,* vol. 1, 2021.

[3] P. P. Singh, A. Jaswal, R. Singh, T. Mondal, and K. K. Pant, "Green hydrogen production from biomass – A thermodynamic assessment of the potential of conventional and advanced bio-oil steam reforming processes," *International Journal of Hydrogen Energy,* vol. 50, pp. 627-639, 2024/01/02/ 2024, doi: https://doi.org/10.1016/j.ijhydene.2023.10.099.

[4] M. Byun, B. Lee, H. Lee, S. Jung, H. Ji, and H. Lim, "Techno-economic and environmental assessment of methanol steam reforming for H2 production at various scales," *International Journal of Hydrogen Energy,* vol. 45, no. 46, pp. 24146-24158, 2020/09/21/ 2020, doi: https://doi.org/10.1016/j.ijhydene.2020.06.097.

[5] S. Galera and F. J. Gutiérrez Ortiz, "Techno-economic assessment of hydrogen and power production from supercritical water reforming of glycerol," *Fuel,* vol. 144, pp. 307-316, 2015/03/15/ 2015, doi: https://doi.org/10.1016/j.fuel.2014.12.033.

[6] T. Lepage, M. Kammoun, Q. Schmetz, and A. Richel, "Biomass-to-hydrogen: A review of main routes production, processes evaluation and techno-economical assessment," *Biomass and Bioenergy,* vol. 144, p. 105920, 2021/01/01/ 2021, doi: https://doi.org/10.1016/j.biombioe.2020.105920.

[7] IEA, "Global Hydrogen Review 2024," IEA, Paris, 2024. [Online]. Available: https://www.iea.org/reports/global-hydrogen-review-2024

[8] R. L. Edwards, C. Font-Palma, and J. Howe, "The status of hydrogen technologies in the UK: A multi-disciplinary review," *Sustainable Energy Technologies and Assessments,* vol. 43, p. 100901, 2021/02/01/ 2021, doi: https://doi.org/10.1016/j.seta.2020.100901.

[9] M. H. Ali Khan, R. Daiyan, P. Neal, N. Haque, I. MacGill, and R. Amal, "A framework for assessing economics of blue hydrogen production from steam methane reforming using carbon capture storage & utilisation," *International Journal of Hydrogen Energy,* vol. 46, no.

44, pp. 22685-22706, 2021/06/28/ 2021, doi: https://doi.org/10.1016/j.ijhydene.2021.04.104.

[10] V. H. de Abreu, V. G. Pereira, L. F. Proença, F. S. Toniolo, and A. S. Santos, "A Systematic Study on Techno-Economic Evaluation of Hydrogen Production," *Energies*, vol. 16, no. 18, doi: 10.3390/en16186542.

[11] A. María Villarreal Vives, R. Wang, S. Roy, and A. Smallbone, "Techno-economic analysis of large-scale green hydrogen production and storage," *Applied Energy,* vol. 346, p. 121333, 2023/09/15/ 2023, doi: https://doi.org/10.1016/j.apenergy.2023.121333.

[12] M. R. Shaner, H. A. Atwater, N. S. Lewis, and E. W. McFarland, "A comparative technoeconomic analysis of renewable hydrogen production using solar energy," *Energy & Environmental Science,* 10.1039/C5EE02573G vol. 9, no. 7, pp. 2354-2371, 2016, doi: 10.1039/C5EE02573G.

[13] A. Henry, D. McStay, D. Rooney, P. Robertson, and A. Foley, "Techno-economic analysis to identify the optimal conditions for green hydrogen production," *Energy Conversion and Management,* vol. 291, p. 117230, 2023/09/01/ 2023, doi: https://doi.org/10.1016/j.enconman.2023.117230.

[14] A. Liponi, A. Baccioli, L. Ferrari, and U. Desideri, "Techno-economic analysis of hydrogen production from PV plants," in *E3S web of conferences*, 2022, vol. 334: EDP Sciences, p. 01001.

[15] M. Younas, S. Shafique, A. Hafeez, F. Javed, and F. Rehman, "An Overview of Hydrogen Production: Current Status, Potential, and Challenges," *Fuel,* vol. 316, p. 123317, 2022/05/15/ 2022, doi: https://doi.org/10.1016/j.fuel.2022.123317.

[16] M. A. Qyyum *et al.*, "Availability, versatility, and viability of feedstocks for hydrogen production: Product space perspective," *Renewable and Sustainable Energy Reviews,* vol. 145, p. 110843, 2021/07/01/ 2021, doi: https://doi.org/10.1016/j.rser.2021.110843.

[17] H. R. Sara, B. Enrico, V. Mauro, D. C. Andrea, and N. Vincenzo, "Techno-economic Analysis of Hydrogen Production Using Biomass Gasification -A Small Scale Power Plant Study," *Energy*

Procedia, vol. 101, pp. 806-813, 2016/11/01/ 2016, doi: https://doi.org/10.1016/j.egypro.2016.11.102.

[18] H. Song *et al.*, "Recent development of biomass gasification for H2 rich gas production," *Applications in Energy and Combustion Science,* vol. 10, p. 100059, 2022/06/01/ 2022, doi: https://doi.org/10.1016/j.jaecs.2022.100059.

[19] M. A. Soria, D. Barros, and L. M. Madeira, "Hydrogen production through steam reforming of bio-oils derived from biomass pyrolysis: Thermodynamic analysis including in situ CO2 and/or H2 separation," *Fuel,* vol. 244, pp. 184-195, 2019/05/15/ 2019, doi: https://doi.org/10.1016/j.fuel.2019.01.156.

[20] M. Imizcoz and A. V. Puga, "Assessment of Photocatalytic Hydrogen Production from Biomass or Wastewaters Depending on the Metal Co-Catalyst and Its Deposition Method on TiO2," *Catalysts*, vol. 9, no. 7*,* doi: 10.3390/catal9070584.

[21] T. Keskin, M. Gungormusler, B. Bayar, and H. N. Abubackar, "Chapter 17 - Biohydrogen production by biological water-gas shift reaction and bioelectrochemical systems," in *Bioenergy Engineering*, K. P. Shadangi, P. K. Sarangi, K. Mohanty, I. Deniz, and A. R. Kiran Gollakota Eds.: Woodhead Publishing, 2023, pp. 353-380.

[22] R. Łukajtis *et al.*, "Hydrogen production from biomass using dark fermentation," *Renewable and Sustainable Energy Reviews,* vol. 91, pp. 665-694, 2018/08/01/ 2018, doi: https://doi.org/10.1016/j.rser.2018.04.043.

[23] S. Gadkari *et al.*, "Techno-Economic Analysis of 2,3-Butanediol Production from Sugarcane Bagasse," *ACS Sustainable Chemistry & Engineering,* vol. 11, no. 22, pp. 8337-8349, 2023/06/05 2023, doi: 10.1021/acssuschemeng.3c01221.

[24] S. Chatterjee and S. Venkata Mohan, "Simultaneous production of green hydrogen and bioethanol from segregated sugarcane bagasse hydrolysate streams with circular biorefinery design," *Chemical Engineering Journal,* vol. 425, p. 130386, 2021/12/01/ 2021, doi: https://doi.org/10.1016/j.cej.2021.130386.

[25] M. Munagala, Y. Shastri, K. Nalawade, K. Konde, and S. Patil, "Life cycle and economic assessment of sugarcane bagasse valorization to lactic acid," *Waste Management,* vol. 126, pp. 52-64, 2021/05/01/ 2021, doi: https://doi.org/10.1016/j.wasman.2021.02.052.

[26] N. Cirqueira, E. de Souza Candeo, L. Barboza, F. Troyner, J. Martins Teixeira de Abreu Pietrobelli, and E. Bittencourt Sydney, "Sugarcane First-Generation Bioethanol Units and Advancements in Electric Power and Biogas Production," in *Liquid Biofuels: Bioethanol*, C. R. Soccol, G. Amarante Guimarães Pereira, C.-G. Dussap, and L. Porto de Souza Vandenberghe Eds. Cham: Springer International Publishing, 2022, pp. 85-107.

[27] R. H. Hafyan *et al.*, "Integrated biorefinery for bioethanol and succinic acid co-production from bread waste: Techno-economic feasibility and life cycle assessment," *Energy Conversion and Management,* vol. 301, p. 118033, 2024/02/01/ 2024, doi: https://doi.org/10.1016/j.enconman.2023.118033.

[28] V. Kumar *et al.*, "Bread waste – A potential feedstock for sustainable circular biorefineries," *Bioresource Technology,* vol. 369, p. 128449, 2023/02/01/ 2023, doi: https://doi.org/10.1016/j.biortech.2022.128449.

[29] V. Narisetty *et al.*, "Recycling bread waste into chemical building blocks using a circular biorefining approach," *Sustainable Energy & Fuels,* vol. 5, no. 19, pp. 4842-4849, 2021.

[30] V. Kumar *et al.*, "Bread waste–A potential feedstock for sustainable circular biorefineries," *Bioresource technology,* p. 128449, 2022.

[31] V. Narisetty *et al.*, "Process optimization for recycling of bread waste into bioethanol and biomethane: A circular economy approach," *Energy Conversion and Management,* vol. 266, p. 115784, 2022/08/15/ 2022, doi: https://doi.org/10.1016/j.enconman.2022.115784.

[32] C. C. J. Leung, A. S. Y. Cheung, A. Y.-Z. Zhang, K. F. Lam, and C. S. K. Lin, "Utilisation of waste bread for fermentative succinic acid production," *Biochemical Engineering Journal,* vol. 65, pp. 10-15, 2012/06/15/ 2012, doi: https://doi.org/10.1016/j.bej.2012.03.010.

[33] R. Cox *et al.*, "High-Level fermentative production of Lactic acid from bread waste under Non-sterile conditions with a circular biorefining approach and zero waste discharge," *Fuel,* vol. 313, p. 122976, 2022/04/01/ 2022, doi: https://doi.org/10.1016/j.fuel.2021.122976.

[34] V. Narisetty *et al.*, "Fermentative production of 2,3-Butanediol using bread waste – A green approach for sustainable management of food waste," *Bioresource Technology,* vol. 358, p. 127381, 2022/08/01/ 2022, doi: https://doi.org/10.1016/j.biortech.2022.127381.

[35] L. V. Mattos, G. Jacobs, B. H. Davis, and F. B. Noronha, "Production of Hydrogen from Ethanol: Review of Reaction Mechanism and Catalyst Deactivation," *Chemical Reviews,* vol. 112, no. 7, pp. 4094-4123, 2012/07/11 2012, doi: 10.1021/cr2000114.

[36] Z. Ferencz *et al.*, "Effects of Support and Rh Additive on Co-Based Catalysts in the Ethanol Steam Reforming Reaction," *ACS Catalysis,* vol. 4, no. 4, pp. 1205-1218, 2014/04/04 2014, doi: 10.1021/cs500045z.

[37] I. Rossetti, M. Compagnoni, and M. Torli, "Process simulation and optimisation of H2 production from ethanol steam reforming and its use in fuel cells. 1. Thermodynamic and kinetic analysis," *Chemical Engineering Journal,* vol. 281, pp. 1024-1035, 2015/12/01/ 2015, doi: https://doi.org/10.1016/j.cej.2015.08.025.

[38] A. Baig, S. Dhanushkar, and Sonal, "Coke-resistant lanthana promoted Ni/CeO2-ZrO2 catalysts for hydrogen generation via ethanol steam reforming," *Gas Science and Engineering,* p. 205537, 2025/01/04/ 2025, doi: https://doi.org/10.1016/j.jgsce.2025.205537.

[39] S. Roychowdhury, M. Mukthar Ali, S. Dhua, T. Sundararajan, and G. Ranga Rao, "Thermochemical hydrogen production using Rh/CeO2/γ-Al2O3 catalyst by steam reforming of ethanol and water splitting in a packed bed reactor," *International Journal of Hydrogen Energy,* vol. 46, no. 37, pp. 19254-19269, 2021/05/28/ 2021, doi: https://doi.org/10.1016/j.ijhydene.2021.03.079.

[40] M. Compagnoni, E. Mostafavi, A. Tripodi, N. Mahinpey, and I. Rossetti, "Techno-economic Analysis of a Bioethanol to Hydrogen Centralized Plant," *Energy & Fuels,* vol. 31, no. 11, pp. 12988-12996, 2017/11/16 2017, doi: 10.1021/acs.energyfuels.7b02434.

[41] T. S. Moraes *et al.*, "A techno-economic evaluation of the hydrogen production for energy generation using an ethanol fuel processor," *International Journal of Hydrogen Energy,* vol. 44, no. 39, pp. 21205-21219, 2019/08/13/ 2019, doi: https://doi.org/10.1016/j.ijhydene.2019.06.182.

[42] P. Khamhaeng, N. Laosiripojana, S. Assabumrungrat, and P. Kim-Lohsoontorn, "Techno-economic analysis of hydrogen production from dehydrogenation and steam reforming of ethanol for carbon dioxide conversion to methanol," *International Journal of Hydrogen Energy,* vol. 46, no. 60, pp. 30891-30902, 2021/09/01/ 2021, doi: https://doi.org/10.1016/j.ijhydene.2021.04.048.

[43] A. Fasolini, R. Cucciniello, E. Paone, F. Mauriello, and T. Tabanelli, "A Short Overview on the Hydrogen Production Via Aqueous Phase Reforming (APR) of Cellulose, C6-C5 Sugars and Polyols," *Catalysts*, vol. 9, no. 11*,* doi: 10.3390/catal9110917.

[44] A. N. Joshi and P. D. Vaidya, "Recent studies on aqueous-phase reforming: Catalysts, reactors, hybrid processes and techno-economic analysis," *International Journal of Hydrogen Energy,* vol. 49, pp. 117-137, 2024/01/02/ 2024, doi: https://doi.org/10.1016/j.ijhydene.2023.06.314.

[45] T. Jiang, T. Wang, L. Ma, Y. Li, Q. Zhang, and X. Zhang, "Investigation on the xylitol aqueous-phase reforming performance for pentane production over Pt/HZSM-5 and Ni/HZSM-5 catalysts," *Applied Energy,* vol. 90, no. 1, pp. 51-57, 2012/02/01/ 2012, doi: https://doi.org/10.1016/j.apenergy.2011.03.034.

[46] A. V. Kirilin *et al.*, "Aqueous-phase reforming of xylitol over Pt/C and Pt/TiC-CDC catalysts: catalyst characterization and catalytic performance," *Catalysis Science & Technology,* 10.1039/C3CY00636K vol. 4, no. 2, pp. 387-401, 2014, doi: 10.1039/C3CY00636K.

[47] H. A. Duarte, M. E. Sad, and C. R. Apesteguía, "Production of bio-hydrogen by liquid processing of xylitol on Pt/Al2O3 catalysts: Effect of the metal loading," *International Journal of Hydrogen Energy,* vol. 42, no. 7, pp. 4051-4060, 2017/02/16/ 2017, doi: https://doi.org/10.1016/j.ijhydene.2016.11.119.

[48] D. Y. Murzin *et al.*, "Kinetics, Modeling, and Process Design of Hydrogen Production by Aqueous Phase Reforming of Xylitol," *Industrial & Engineering Chemistry Research,* vol. 56, no. 45, pp. 13240-13253, 2017/11/15 2017, doi: 10.1021/acs.iecr.7b01636.

[49] L. I. Godina, A. V. Kirilin, A. V. Tokarev, I. L. Simakova, and D. Y. Murzin, "Sibunit-Supported Mono- and Bimetallic Catalysts Used in Aqueous-Phase Reforming of Xylitol," *Industrial & Engineering Chemistry Research,* vol. 57, no. 6, pp. 2050-2067, 2018/02/14 2018, doi: 10.1021/acs.iecr.7b04937.

[50] M. Khodabandehloo, A. Larimi, and F. Khorasheh, "Comparative process modeling and techno-economic evaluation of renewable hydrogen production by glycerol reforming in aqueous and gaseous phases," *Energy Conversion and Management,* vol. 225, p. 113483, 2020/12/01/ 2020, doi: https://doi.org/10.1016/j.enconman.2020.113483.

[51] D. A. Sladkovskiy, L. I. Godina, K. V. Semikin, E. V. Sladkovskaya, D. A. Smirnova, and D. Y. Murzin, "Process design and techno-economical analysis of hydrogen production by aqueous phase reforming of sorbitol," *Chemical Engineering Research and Design,* vol. 134, pp. 104-116, 2018/06/01/ 2018, doi: https://doi.org/10.1016/j.cherd.2018.03.041.

[52] Y. Mordechai Koskas, A. Golberg, M. Gozin, and A. Kribus, "Process simulation for mass balance of continuous biomass hydrothermal liquefaction with reaction kinetics," *Energy Conversion and Management: X,* vol. 20, p. 100477, 2023/10/01/ 2023, doi: https://doi.org/10.1016/j.ecmx.2023.100477.

[53] A. N. C. H. Wee, A. E. Erison, E. H. Edward Anyek, G. R. Pakpahan, J. R. Lim, and A. N. T. Tiong, "Techno-economic assessment of hydrogen production via steam reforming of palm oil mill

effluent," *Sustainable Energy Technologies and Assessments,* vol. 53, p. 102575, 2022/10/01/ 2022, doi: https://doi.org/10.1016/j.seta.2022.102575.

[54] Y. Yan, V. Manovic, E. J. Anthony, and P. T. Clough, "Techno-economic analysis of low-carbon hydrogen production by sorption enhanced steam methane reforming (SE-SMR) processes," *Energy Conversion and Management,* vol. 226, p. 113530, 2020/12/15/ 2020, doi: https://doi.org/10.1016/j.enconman.2020.113530.

[55] D. Humbird *et al.*, "Process design and economics for biochemical conversion of lignocellulosic biomass to ethanol: dilute-acid pretreatment and enzymatic hydrolysis of corn stover," National Renewable Energy Lab.(NREL), Golden, CO (United States), 2011.

[56] G. Franceschin, M. Sudiro, T. Ingram, I. Smirnova, G. Brunner, and A. Bertucco, "Conversion of rye straw into fuel and xylitol: a technical and economical assessment based on experimental data," *Chemical Engineering Research and Design,* vol. 89, no. 6, pp. 631-640, 2011/06/01/ 2011, doi: https://doi.org/10.1016/j.cherd.2010.11.001.

[57] G. Galán, M. Martín, and I. E. Grossmann, "Integrated Renewable Production of Sorbitol and Xylitol from Switchgrass," *Industrial & Engineering Chemistry Research,* vol. 60, no. 15, pp. 5558-5573, 2021/04/21 2021, doi: 10.1021/acs.iecr.1c00397.

[58] T. Morakile, M. Mandegari, S. Farzad, and J. F. Görgens, "Comparative techno-economic assessment of sugarcane biorefineries producing glutamic acid, levulinic acid and xylitol from sugarcane," *Industrial Crops and Products,* vol. 184, p. 115053, 2022/09/15/ 2022, doi: https://doi.org/10.1016/j.indcrop.2022.115053.

[59] H. M. R. Özüdoğru, M. Nieder-Heitmann, K. F. Haigh, and J. F. Görgens, "Techno-economic analysis of product biorefineries utilizing sugarcane lignocelluloses: Xylitol, citric acid and glutamic acid scenarios annexed to sugar mills with electricity co-production," *Industrial Crops and Products,* vol. 133, pp. 259-268, 2019/07/01/ 2019, doi: https://doi.org/10.1016/j.indcrop.2019.03.015.

[60] G. V. S. Seufitelli, H. El-Husseini, D. U. Pascoli, R. Bura, and R. Gustafson, "Techno-economic analysis of an integrated biorefinery to convert poplar into jet fuel, xylitol, and formic acid," *Biotechnology for Biofuels and Bioproducts,* vol. 15, no. 1, p. 143, 2022/12/20 2022, doi: 10.1186/s13068-022-02246-3.

[61] A. D. Mountraki, K. R. Koutsospyros, B. B. Mlayah, and A. C. Kokossis, "Selection of Biorefinery Routes: The Case of Xylitol and its Integration with an Organosolv Process," *Waste and Biomass Valorization,* vol. 8, no. 7, pp. 2283-2300, 2017/10/01 2017, doi: 10.1007/s12649-016-9814-8.

[62] J.-P. Mikkola *et al.*, "Hydrogenation of xylose to xylitol on sponge nickel catalyst: a study of the process and catalyst deactivation kinetics," *Brazilian Journal of Chemical Engineering,* vol. 20, pp. 263-271, 2003.

[63] K. L. Gerbrandt, *The Impacts of Xylitol Production from Hemicellulose Residues: Process Design, Life Cycle, and Techno-Economic Assessment*. University of Toronto (Canada), 2014.

[64] V. Hernández, J. M. Romero-García, J. A. Dávila, E. Castro, and C. A. Cardona, "Techno-economic and environmental assessment of an olive stone based biorefinery," *Resources, Conservation and Recycling,* vol. 92, pp. 145-150, 2014/11/01/ 2014, doi: https://doi.org/10.1016/j.resconrec.2014.09.008.

[65] B. Lamolinara, A. Pérez-Martínez, E. Guardado-Yordi, C. Guillén Fiallos, K. Diéguez-Santana, and G. J. Ruiz-Mercado, "Anaerobic digestate management, environmental impacts, and techno-economic challenges," *Waste Management,* vol. 140, pp. 14-30, 2022/03/01/ 2022, doi: https://doi.org/10.1016/j.wasman.2021.12.035.

[66] T. Y. Chong *et al.*, "Techno-economic evaluation of third-generation bioethanol production utilizing the macroalgae waste: A case study in Malaysia," *Energy,* vol. 210, p. 118491, 2020/11/01/ 2020, doi: https://doi.org/10.1016/j.energy.2020.118491.

[67] S. S. Hla *et al.*, "Kinetics of high-temperature water-gas shift reaction over two iron-based commercial catalysts using simulated coal-derived syngases," *Chemical Engineering Journal,*

vol. 146, no. 1, pp. 148-154, 2009/01/15/ 2009, doi: https://doi.org/10.1016/j.cej.2008.09.023.

[68] Y. Choi and H. G. Stenger, "Water gas shift reaction kinetics and reactor modeling for fuel cell grade hydrogen," *Journal of Power Sources,* vol. 124, no. 2, pp. 432-439, 2003/11/24/ 2003, doi: https://doi.org/10.1016/S0378-7753(03)00614-1.

[69] J. Zhang, N. Fatah, S. Capela, Y. Kara, O. Guerrini, and A. Y. Khodakov, "Kinetic investigation of carbon monoxide hydrogenation under realistic conditions of methanation of biomass derived syngas," *Fuel,* vol. 111, pp. 845-854, 2013/09/01/ 2013, doi: https://doi.org/10.1016/j.fuel.2013.04.057.

[70] A. Devi, A. Niazi, M. Ramteke, and S. Upadhyayula, "Techno-economic analysis of ethanol production from lignocellulosic biomass–a comparison of fermentation, thermo catalytic, and chemocatalytic technologies," *Bioprocess and Biosystems Engineering,* vol. 44, no. 6, pp. 1093-1107, 2021/06/01 2021, doi: 10.1007/s00449-020-02504-4.

[71] A. Zohrabian, M. Mansouri Majoumerd, M. Soltanieh, and S. Sattari, "Techno-economic evaluation of an integrated hydrogen and power co-generation system with CO2 capture," *International Journal of Greenhouse Gas Control,* vol. 44, pp. 94-103, 2016/01/01/ 2016, doi: https://doi.org/10.1016/j.ijggc.2015.11.004.

[72] S. M. Hosseini-Ardali, M. Hazrati-Kalbibaki, M. Fattahi, and F. Lezsovits, "Multi-objective optimization of post combustion CO2 capture using methyldiethanolamine (MDEA) and piperazine (PZ) bi-solvent," *Energy,* vol. 211, p. 119035, 2020/11/15/ 2020, doi: https://doi.org/10.1016/j.energy.2020.119035.

[73] H. B. Carminati, R. d. F. D. Milão, J. L. de Medeiros, and O. d. Q. F. Araújo, "Bioenergy and full carbon dioxide sinking in sugarcane-biorefinery with post-combustion capture and storage: Techno-economic feasibility," *Applied Energy,* vol. 254, p. 113633, 2019/11/15/ 2019, doi: https://doi.org/10.1016/j.apenergy.2019.113633.

[74] M. Malekli, A. Aslani, Z. Zolfaghari, and R. Zahedi, "CO2 capture and sequestration from a mixture of direct air and industrial exhaust gases using MDEA/PZ: Optimal design by process integration with organic rankine cycle," *Energy Reports,* vol. 9, pp. 4701-4712, 2023/12/01/ 2023, doi: https://doi.org/10.1016/j.egyr.2023.03.115.

[75] R. Junsittiwate, T. R. Srinophakun, and S. Sukpancharoen, "Techno-economic, environmental, and heat integration of palm empty fruit bunch upgrading for power generation," *Energy for Sustainable Development,* vol. 66, pp. 140-150, 2022/02/01/ 2022, doi: https://doi.org/10.1016/j.esd.2021.12.001.

[76] J. Sadhukhan, K. S. Ng, and E. M. Hernandez, *Biorefineries and chemical processes: design, integration and sustainability analysis* (Economic Analysis). John Wiley & Sons, 2014.

[77] M. S. Peters, K. D. Timmerhaus, and R. E. West, *Plant design and economics for chemical engineers*. McGraw-Hill New York, 2003.

[78] J. A. Quintero and C. A. Cardona, "Process Simulation of Fuel Ethanol Production from Lignocellulosics using Aspen Plus," *Industrial & Engineering Chemistry Research,* vol. 50, no. 10, pp. 6205-6212, 2011/05/18 2011, doi: 10.1021/ie101767x.

[79] S. Mailaram *et al.*, "Lactic acid and biomethane production from bread waste: a techno-economic and profitability analysis using pinch technology," *Sustainable Energy & Fuels,* 10.1039/D3SE00119A vol. 7, no. 13, pp. 3034-3046, 2023, doi: 10.1039/D3SE00119A.

[80] V. Spallina, G. Motamedi, F. Gallucci, and M. van Sint Annaland, "Techno-economic assessment of an integrated high pressure chemical-looping process with packed-bed reactors in large scale hydrogen and methanol production," *International Journal of Greenhouse Gas Control,* vol. 88, pp. 71-84, 2019/09/01/ 2019, doi: https://doi.org/10.1016/j.ijggc.2019.05.026.

[81] M. Melikoglu and A. Tekin, "Biohydrogen production from food and agricultural wastes: A global review and a techno-economic evaluation for Turkey," *International Journal of*

Hydrogen Energy, vol. 62, pp. 913-924, 2024/04/10/ 2024, doi: https://doi.org/10.1016/j.ijhydene.2024.03.173.

[82] S. Banerjee, M. Munagala, Y. Shastri, R. Vijayaraghavan, A. F. Patti, and A. Arora, "Process Design and Techno-Economic Feasibility Analysis of an Integrated Pineapple Processing Waste Biorefinery," *ACS Engineering Au,* vol. 2, no. 3, pp. 208-218, 2022/06/15 2022, doi: 10.1021/acsengineeringau.1c00028.

[83] F. Regis, A. H. A. Monteverde, and D. Fino, "A techno-economic assessment of bioethanol production from switchgrass through biomass gasification and syngas fermentation," *Energy,* vol. 274, p. 127318, 2023/07/01/ 2023, doi: https://doi.org/10.1016/j.energy.2023.127318.

[84] P. Thanahiranya *et al.*, "Succinic Acid Production from Glycerol by Actinobacillus succinogenes: Techno-economic, environmental, and exergy analyses," *Journal of Cleaner Production,* vol. 404, p. 136927, 2023/06/10/ 2023, doi: https://doi.org/10.1016/j.jclepro.2023.136927.

[85] K. Wiranarongkorn, K. Im-orb, Y. Patcharavorachot, F. Maréchal, and A. Arpornwichanop, "Comparative techno-economic and energy analyses of integrated biorefinery processes of furfural and 5-hydroxymethylfurfural from biomass residue," *Renewable and Sustainable Energy Reviews,* vol. 175, p. 113146, 2023/04/01/ 2023, doi: https://doi.org/10.1016/j.rser.2023.113146.

[86] D. J. Nouwe Edou and J. A. Onwudili, "Comparative techno-economic modelling of large-scale thermochemical biohydrogen production technologies to fuel public buses: A case study of West Midlands region of England," *Renewable Energy,* vol. 189, pp. 704-716, 2022/04/01/ 2022, doi: https://doi.org/10.1016/j.renene.2022.02.074.

[87] Y. Li, Y. Han, Y. Zhang, W. Luo, and G. Li, "Anaerobic digestion of different agricultural wastes: A techno-economic assessment," *Bioresource Technology,* vol. 315, p. 123836, 2020/11/01/ 2020, doi: https://doi.org/10.1016/j.biortech.2020.123836.

[88] V. Gubin *et al.*, "Hydrogen production from woody biomass gasification: a techno-economic analysis," *Biofuels, Bioproducts and Biorefining,* vol. 18, no. 4, pp. 818-836, 2024/07/01 2024, doi: https://doi.org/10.1002/bbb.2647.

[89] C. Zhao, J. Huang, D. Xie, Y. Qiao, and M. Xu, "Thermodynamic and techno-economic analysis of hydrogen production from food waste by torrefaction integrated with steam gasification," *Energy Conversion and Management,* vol. 299, p. 117826, 2024/01/01/ 2024, doi: https://doi.org/10.1016/j.enconman.2023.117826.

[90] P. Parthasarathy, K. S. Narayanan, S. Ceylan, and N. A. Pambudi, "Optimization of Parameters for the Generation of Hydrogen in Combined Slow Pyrolysis and Steam Gasification of Biomass," *Energy & Fuels,* vol. 31, no. 12, pp. 13692-13704, 2017/12/21 2017, doi: 10.1021/acs.energyfuels.7b02429.

[91] A. Arregi, G. Lopez, M. Amutio, I. Barbarias, J. Bilbao, and M. Olazar, "Hydrogen production from biomass by continuous fast pyrolysis and in-line steam reforming," *RSC Advances,* 10.1039/C6RA01657J vol. 6, no. 31, pp. 25975-25985, 2016, doi: 10.1039/C6RA01657J.

[92] L. J. Swart, A. M. Petersen, O. K. K. Bedzo, and J. F. Görgens, "Techno-economic analysis of the valorization of brewers spent grains: production of xylitol and xylo-oligosaccharides," *Journal of Chemical Technology & Biotechnology,* vol. 96, no. 6, pp. 1632-1644, 2021/06/01 2021, doi: https://doi.org/10.1002/jctb.6683.

[93] M. El Ibrahimi, I. Khay, A. El Maakoul, and M. Bakhouya, "Techno-economic and environmental assessment of anaerobic co-digestion plants under different energy scenarios: A case study in Morocco," *Energy Conversion and Management,* vol. 245, p. 114553, 2021/10/01/ 2021, doi: https://doi.org/10.1016/j.enconman.2021.114553.

[94] W. Y. Hong, "A techno-economic review on carbon capture, utilisation and storage systems for achieving a net-zero CO2 emissions future," *Carbon Capture Science & Technology,* vol. 3, p. 100044, 2022/06/01/ 2022, doi: https://doi.org/10.1016/j.ccst.2022.100044.

[95] B. Cook and C. Hagen, "Techno-economic analysis of biomass gasification for hydrogen production in three US-based case studies," *International Journal of Hydrogen Energy,* vol. 49, pp. 202-218, 2024/01/02/ 2024, doi: https://doi.org/10.1016/j.ijhydene.2023.07.219.

[96] D. Schweitzer *et al.*, "Process simulation and techno-economic assessment of SER steam gasification for hydrogen production," *International Journal of Hydrogen Energy,* vol. 43, no. 2, pp. 569-579, 2018/01/11/ 2018, doi: https://doi.org/10.1016/j.ijhydene.2017.11.001.

[97] C.-C. Cormos, "Green hydrogen production from decarbonized biomass gasification: An integrated techno-economic and environmental analysis," *Energy,* vol. 270, p. 126926, 2023/05/01/ 2023, doi: https://doi.org/10.1016/j.energy.2023.126926.

[98] Y. K. Salkuyeh, B. A. Saville, and H. L. MacLean, "Techno-economic analysis and life cycle assessment of hydrogen production from different biomass gasification processes," *International Journal of Hydrogen Energy,* vol. 43, no. 20, pp. 9514-9528, 2018/05/17/ 2018, doi: https://doi.org/10.1016/j.ijhydene.2018.04.024.

[99] N. Wu, K. Lan, and Y. Yao, "An integrated techno-economic and environmental assessment for carbon capture in hydrogen production by biomass gasification," *Resources, Conservation and Recycling,* vol. 188, p. 106693, 2023/01/01/ 2023, doi: https://doi.org/10.1016/j.resconrec.2022.106693.

[100] J. Hong, B. Chen, T. Wang, and X. Zhao, "A promising technical route for converting lignocellulose to bio-jet fuels based on bioconversion of biomass and coupling of aqueous ethanol: A techno-economic assessment," *Fuel,* vol. 381, p. 133670, 2025/02/01/ 2025, doi: https://doi.org/10.1016/j.fuel.2024.133670.

[101] Q. Qian, Z. Luo, H. Sun, Q. Wei, J. Shi, and L. Li, "Life cycle assessment and techno-economic analysis of wood-based biorefineries for cellulosic ethanol production," *Bioresource Technology,* vol. 399, p. 130595, 2024/05/01/ 2024, doi: https://doi.org/10.1016/j.biortech.2024.130595.

[102] R. Ren, H. Wang, X. Feng, and C. You, "Techno-economic analysis of auto-thermal gasification of municipal solid waste with ash direct melting for hydrogen production," *Energy Conversion and Management,* vol. 292, p. 117401, 2023/09/15/ 2023, doi: https://doi.org/10.1016/j.enconman.2023.117401.

[103] C. Yilmaz, S. N. Ozdemir, U. Kocak, and N. Tokgoz, "Techno-economic analysis and experimental validation of solar-assisted low-temperature water electrolysis for green hydrogen production: Insights from Afyonkarahisar," *Fuel,* vol. 383, p. 133762, 2025/03/01/ 2025, doi: https://doi.org/10.1016/j.fuel.2024.133762.

[104] B. Parkinson *et al.*, "Hydrogen production using methane: Techno-economics of decarbonizing fuels and chemicals," *International Journal of Hydrogen Energy,* vol. 43, no. 5, pp. 2540-2555, 2018/02/01/ 2018, doi: https://doi.org/10.1016/j.ijhydene.2017.12.081.

[105] A. Pettinau, D. Marotto, F. Dessì, and F. Ferrara, "Techno-economic assessment of renewable hydrogen production for mobility: A case study," *Energy Conversion and Management,* vol. 311, p. 118513, 2024/07/01/ 2024, doi: https://doi.org/10.1016/j.enconman.2024.118513.

[106] W. Han, Y. Y. Hu, S. Y. Li, F. F. Li, and J. H. Tang, "Biohydrogen production from waste bread in a continuous stirred tank reactor: A techno-economic analysis," *Bioresource Technology,* vol. 221, pp. 318-323, 2016/12/01/ 2016, doi: https://doi.org/10.1016/j.biortech.2016.09.055.

[107] R. H. Hafyan *et al.*, "Bread waste valorization: a review of sustainability aspects and challenges," (in English), *Frontiers in Sustainable Food Systems,* Review vol. 8, 2024-February-05 2024, doi: 10.3389/fsufs.2024.1334801.

DSPACE

https://dspace.org/

A comparative techno-economic feasibility of hydrogen production from sugarcane bagasse and bread waste

Hafyan, Rendra Hakim; Sadhukhan, Jhuma; Kumar, Vinod; Maity, Sunil K.; Gadkari, Siddharth

2025-05-15
Elsevier
https://doi.org/10.1016/j.fuel.2025.134469
Hafyan RH, Sadhukhan J, Kumar V, et al., (2025) A comparative techno-economic feasibility of hydrogen production from sugarcane bagasse and bread waste. Fuel, Volume 388, May 2025, Article number 134469

Downloaded from a DSpace repository. https://dspace.org/